

NPS ARCHIVE
1962.06
GERHAN, C.



THE COLLEGE OF AERONAUTICS
CRANFIELD

THESIS

TITLE: A SIMPLIFIED APPROACH
TO LOW HEIGHT
DETERMINATION

NAME:

CHARLES F. GERHAN, JR.

Thesis
G295

DATE 4 JUNE 1962

A SIMPLIFIED APPROACH TO LOW HEIGHT DETERMINATION

SUMMARY

In this report a method of height determination using ground reflected energy is analyzed and the results of relevant tests performed are reported and discussed. The approach considered differs from conventional radio altimetry in that time delay measurement is not employed. The simplicity of required equipment suggests the likelihood of space, weight, and power consumption savings.

As the primary result, it is shown that an oscillator's frequency may be related to the separation between its load antenna and a reflecting surface toward which it is radiating. The resulting relationship is periodic with the frequency alternately deviating positively and

negatively about a center value. The center frequency occurs at quarter wave length intervals in antenna-to-reflecting surface separation. The height information available is less than that obtained from a conventional radio altimeter, but it may be useful in some applications.

The content of this report consists of the thesis of a student in the Diploma course at the College of Aeronautics, Cranfield, England.

The College of Aeronautics
Cranfield, England

13 July 1962

From: LT Charles F. Gerhan, Jr., USN.
To: Superintendent, U. S. Naval Postgraduate
School, Monterey, California.

Subj: College of Aeronautics Thesis, Submission of

1. In accordance with Naval Postgraduate School instructions for officers studying at other institutions, two copies of the thesis prepared by this officer in connection with the Diploma course at the College of Aeronautics are submitted. The second copy was prepared for further transmittal to the Bureau of Naval Weapons as required.

2. The work reported in this thesis entailed a combined theoretical and experimental investigation of the fundamental practicability of a method of height determination based on antenna admittance changes and frequency pulling. The work was performed with the facilities and guidance of the Department of Electrical and Control Engineering, College of Aeronautics, Cranfield, England.

3. The investigations indicated that such a method would be feasible in situations where a requirement exists only for height error information from some predetermined level, rather than continuous height information. The investigations also showed the relative importance of several system parameters, and the report describes the consideration which ought to be given these in a practical system design.

4. After consideration of this thesis and the related oral examination, as well as written examinations on the course undertaken, an assessment of two was made by the College Senate and the Diploma of the College of Aeronautics was awarded.

THE COLLEGE OF AERONAUTICS
CRANFIELD, ENGLAND
DEPARTMENT OF ELECTRICAL AND CONTROL ENGINEERING

THESIS
A SIMPLIFIED APPROACH TO
LOW HEIGHT DETERMINATION

by
Charles F. Gerhan, Jr. B.S.
Lt., U. S. Navy

4th June 1962

TABLE OF CONTENTS

Summary	ii
Introduction	1
Table of Symbols	5
Theory	8
Apparatus	15
Experimental Procedure	24
Results and Discussion	29
System Realization and Application	43
Conclusions	47
Acknowledgements	50
References	51
Appendix I - Input Admittance of the Half Wave Dipole over a Plane Reflecting Surface	53
Appendix II - The Effect of Load on Oscillator Frequency	57
Appendix III - Oscillator Design Calculations	61
Appendix IV - Feeder Length Calculations	64
Tables I - VII	
Figures 1 - 26	

A SIMPLIFIED APPROACH TO LOW HEIGHT DETERMINATION

SUMMARY

In this report a method of height determination using ground reflected energy is analyzed and the results of relevant tests performed are reported and discussed. The approach considered differs from conventional radio altimetry in that time delay measurement is not employed. The simplicity of required equipment suggests the likelihood of space, weight, and power consumption savings.

As the primary result, it is shown that an oscillator's frequency may be related to the separation between its load antenna and a reflecting surface toward which it is radiating. The resulting relationship is periodic with the frequency alternately deviating positively and

negatively about a center value. The center frequency occurs at quarter wave length intervals in antenna-to-reflecting surface separation. The height information available is less than that obtained from a conventional radio altimeter, but it may be useful in some applications.

The content of this report consists of the thesis of a student in the Diploma course at the College of Aeronautics, Cranfield, England.

A SIMPLIFIED APPROACH TO LOW HEIGHT DETERMINATION

INTRODUCTION

Operators of airborne vehicles ordinarily obtain height information by electronic means from a class of equipment called radio or radar altimeters (Ref. 1). Such devices, also known as absolute altimeters or terrain clearance indicators, provide a continuous indication of separation between the vehicle and the underlying terrain. The technique employed is measurement of time delay between radiated and reflected energy parcels, either by pulse or frequency modulation and comparison. Typical performance specifications of such equipment include a range of operation from zero to 5000 feet with an accuracy of plus or minus three per cent but not less than one foot at low heights. Such equipment

commonly consumes a power of two or three hundred watts and weighs about forty pounds. Altimeters of this class have proved entirely satisfactory for general air navigation applications on aircraft large enough to support the physical requirements of the equipment.

For some limited applications, such as the low height determination of a light airborne vehicle, it is likely that the conventional radio altimeter becomes inefficient, in that it is capable of supplying more information than is needed, and does so at the expense of a relatively large requirement in space, weight, and power consumption. The simplified approach to low height determination investigated in this thesis is an attempt to extract a limited, but for certain applications sufficient, amount of height information from a simpler device. As mentioned, the usual radio altimeter utilizes reflected energy for time delay measurement. The approach considered here uses the dependence of antenna input impedance upon this ground reflected energy. Resulting impedance changes appear as load changes to the radio-frequency generator

employed in the system. Such load changes in turn affect the frequency of the generator, so that the frequency provides an analog to the vehicle height above ground. Since only an oscillator, an antenna, a frequency discriminator and connecting cable are required, it is felt that the possibility of space, weight, and power savings is present.

The scope of this work includes an analysis of the phenomena involved and tests of an experimental apparatus employing these principles. The tests conducted were fundamental, since no previous work on a system employing these principles was found.

There were two underlying purposes of the investigations conducted in connection with this thesis. The first purpose was to determine the extent to which the results obtained by a practical application of this approach to low height determination differed from the form of results predicted by the theoretical considerations which are to be discussed. This would include the observation of discrepancies due either to primary effects not considered or higher order

effects which were ignored in the analysis. The second purpose was to gain some familiarity with practical considerations relating to the design of such a system for operational use.

The work was conducted as a Diploma student's thesis in the Department of Electrical and Control Engineering, The College of Aeronautics, Cranfield, England.

TABLE OF SYMBOLS

A	Capacitor disc area; square inches.
a	Depth of rectangular section transmission line; meters.
B	Susceptance normalized to 50 millimhos.
b	Susceptance; mhos (imaginary part of y).
C	Capacitance; farads.
c_{air}	Velocity of propagation in air; approximately 3×10^3 meters per second.
c_{cable}	Velocity of propagation in cable; meters per second.
d	Capacitor plate separation; inches.
$\left. \frac{df}{d\phi} \right]_{\text{line}}$	Reciprocal rate of change of electrical phase on feeder line with frequency; megacycles per second per radian.
$\left. \frac{df}{d\phi} \right]_{\text{osc}}$	Rate of change of oscillator frequency with electrical phase of load; megacycles per second per radian.
e	Voltage measured between accessible terminals; volts.
f	Frequency; cycles per second.
G	Conductance normalized to 50 millimhos.
g	Conductance; mhos (real part of y).

h	Height above ground; inches.
h_{λ}	Height above ground; fractional wave lengths.
i	Current in a circuit; amperes.
j	Square root of -1 .
L	Inductance; henries.
l	Length of cable; meters.
R or r	Resistance; ohms (real part of z).
X	Reactance; ohms (imaginary part of z).
Y	Admittance normalized to 50 millimhos.
y	Admittance; mhos.
y_0	Characteristic admittance of transmission line; mhos.
z	Impedance; ohms.
z_0	Characteristic impedance of transmission line; ohms.
α	Line attenuation constant; nepers per meter.
Δ	Finite increment in prefixed quantity.
ϵ_r	Relative permittivity.
λ_{air}	Wave length in air; meters.
λ_{cable}	Wave length in cable; meters.
μ	Permeability; henries per meter.

- ρ , VSWR Voltage standing wave ratio;
 $\frac{\text{voltage minimum}}{\text{voltage maximum}} ; 0 \leq \rho \leq 1.$
- σ Conductivity; mhos per meter.
- ϕ Electrical phase angle of standing
 wave pattern along feeder cable;
 referred to zero at oscillator
 terminals, positive sense toward
 oscillator; radians (π radians per
 half wave length).

SUBSCRIPTS

- L Load parameters. Conditions at input
 end of short circuited transmission
 line.
- 1, 2 Denotes particular ports in linear
 two-port analysis.

THEORY

This approach to low height determination entails a means of relating height changes to the oscillating frequency of a radio-frequency generator whose energy is directed toward the ground. Two discrete phenomena are involved. First, because of any changes in the distance to the ground, the phase and magnitude of reflected energy returned to the antenna varies, causing a periodic change of antenna input impedance or admittance as a function of height. Second, the impedance or admittance of a load driven by an oscillator determines, to an extent dependent upon the coupling, the parameters of the oscillating circuit and its frequency. Changes in that load will cause the oscillator frequency to shift (to be "pulled") by some amount depending on the amount of the load admittance change and the coupling. These phenomena are linked and made compatible with the desired height-frequency relationship by means of the length of feeder cable connecting the oscillator to the antenna.

To achieve a fundamental insight into the

periodic change of an antenna's admittance over the ground as its height changes, the ideal case of the infinitely thin half wave dipole over a perfectly conducting plane reflecting surface will be considered. Changes of admittance rather than of impedance are chosen so that some comparison with experimental results will be possible, since the equipment used made admittance measurements more convenient. In the experimental system investigated, ideal elements were, of course, not employed. The actual antenna used was not a thin dipole for reasons of experimental flexibility, and the real earth was used as a reflecting surface in order to make predictions about the operational practicability of such a system.

The behavior of the infinitely thin half wave dipole antenna in the vicinity of a perfectly conducting plane reflecting surface can be determined by considering the equivalent system of the same antenna and its image in free space (Ref. 2). The image must be oriented so as to satisfy the boundary condition requiring a vanishing tangential electric vector component

at the reflecting surface. This is achieved in the case of the horizontal dipole by an image dipole of equal length and orientation, displaced from the original antenna by twice the height above the reflecting plane and carrying an oppositely directed and equal current distribution. This arrangement is shown in Fig. 1. In the case where the real earth is the reflecting surface, an image system can still be valid, providing an appropriate change in the image antenna current distribution is made to account for the admittance of the earth. The further development of ideal antenna input admittance changes as a function of height involves the derivation and computation of expressions for the mutual admittance between the image and real antennas as a function of distance between them ($2h$). The results are periodic variations of the real (conductive) and imaginary (susceptive) parts of antenna input admittance as functions of height with amplitudes and phases as shown in Fig. 2. A more complete development is presented in Appendix I.

The dependence of oscillator frequency upon

load and coupling is explained in basic references on electronics (Ref. 3). In Appendix II the particular case of a tuned circuit with capacitor coupled complex load as used in these experiments is discussed. The relationship can be shown graphically in the form of a Rieke diagram for any particular oscillator and coupling combination. In such a presentation, contours of constant frequency and power output appear as functions of load for all possible combinations of complex load admittance. A number of such diagrams are presented in the results of this investigation for the particular oscillator employed.

Two main considerations dictate the choice of feeder length. The antenna in free space will have some definite value of input admittance depending on the geometry of the antenna, the driving frequency, and the characteristic admittance of the feeder transmission line. There will in general be a standing wave pattern on the line. Admittance then varies periodically along the line depending upon the point at which measurement is made, but repeating its values at

half wave length intervals. Thus the feeder must be cut to some integral number of half wave lengths plus that fraction of a half wave length determined by the difference between the antenna free space admittance at operating frequency and the admittance required at the oscillator terminals to produce that operating frequency according to the Rieke diagram. The integral number of half wave lengths of feeder used are chosen based on a different consideration. There is a mutually repetitive relation between electrical feeder length and frequency in this system, since any perturbation in frequency will cause a change of electrical feeder length resulting in a different admittance at the oscillator, hence a further change in frequency. Whether this is stable or not depends on the rate of change of oscillator frequency with electrical phase of the load presented to its terminals as compared with the reciprocal rate of change of electrical phase on the line with frequency (Ref. 4). Fig. 3a shows the case where the combination is stable, as well as the effect of a change in load due to movement of the antenna to a new height above

the ground. Fig. 3b shows the unstable case in which the line is so long that splitting or jumping between two preferential frequencies occurs. Since electrical phase on a transmission line is given by:

$$\phi = \frac{2\pi fl}{c_{\text{cable}}} \quad (1)$$

the rate of change of phase with frequency is

$$\left. \frac{d\phi}{df} \right]_{\text{line}} = \frac{2\pi l}{c_{\text{cable}}} . \quad (2)$$

This is directly dependent on the physical length of cable. For maximum pulling effect without splitting, it is desirable to choose an integral number of half wave lengths to give a slope, $\left. \frac{df}{d\phi} \right]_{\text{line}}$, just greater than that of the oscillator pulling curve at the operating frequency, as in Fig. 3a.

Thus it can be predicted that the result of coupling the antenna, which is a height-to-admittance transducer, to the oscillator, which is an admittance-to-frequency transducer, through the properly selected feeder, which is

an admittance change multiplier, will be a frequency shift directly related to height changes. This, it is expected, will be the key to providing useful height information in a simplified, reliable manner.

APPARATUS

The equipment involved in this investigation consisted of the components of the experimental system being examined, the test apparatus required for determining frequency and admittance, an infinitely variable test load, and the arrangements necessary for supporting the antenna over the ground at various heights.

The antenna was chosen to permit maximum flexibility in oscillator characteristics, and to be sufficiently directive that the effect of nearby surfaces other than the ground directly under it would be kept small. A partially completed suppressed antenna with resonating box was made available from a Swift aircraft being scrapped locally. This antenna was known to have been designed for the frequencies in the neighborhood of 200 megacycles, a band which was desirable from the point of view of having a height range between zero and two or three wave lengths above the ground available conveniently. Construction of the center element and feed point and mounting in a ground plane were necessary

to complete the antenna. The desired result was to obtain a wide range of operating standing wave ratios over a band tunable by a single reasonably stable oscillator. Thus to match a given oscillator characteristic, a wide range of height related phase changes would be available depending upon the operating frequency selected. For convenience in matching with test equipment, a feeder characteristic impedance of 50 ohms was desirable. The lead between the tap point to the active elements and the cable connector was therefore made with Uniradio 67 cable, a 52 ohm line. The tap point and center element width were selected arbitrarily, with later modifications envisaged if required to obtain the desired characteristics. Fig. 4 shows the inside of the resonating box and the back of the antenna with the box cover removed. Fig. 5 illustrates the radiating side of the antenna.

The oscillator was designed based upon a Mullard QOV 03-20A twin tetrode tube which was known to be capable of reasonably good power output in the frequency band considered. Push pull operation with tuned anode and tuned grid

Lecher lines was employed. Provisions were made for tuning by effectively lengthening the lines with adjustable parallel capacitance or shortening them with movable shorting bars. Unbalanced coupling to the load was made through an adjustable capacitor connected to one side of the anode line near the tube anode pin, that being approximately a voltage maximum. A coupling probe was used to obtain a fixed loose coupling as a pick-off for frequency measurements. The tube electrodes were all kept in a floating RF condition by the use of hand wound chokes. A separate regulated laboratory power supply was used for the filament and anode voltages so that the anode voltage could be varied as desired to alter the level of power output. Grid bias was controlled by a potentiometer and 20 pf. capacitor in parallel in the grid circuit. Computations involved in the oscillator design are shown in Appendix III. Since the chosen tube was designed as a neutralized amplifier, and not as an oscillator, it was found necessary to increase the anode to grid feedback by crossover capacitive connections in order to obtain sufficiently

reliable oscillations. This was the main reason for the adjustable shorts on the lines. The original design provided for capacitive tuning over the entire desired frequency range. The added feedback capacitance effectively lengthened the lines, requiring the introduction of shorting bars to compensate. The oscillator is shown in schematic diagram in Fig. 6 and in a photograph in Fig. 7.

The feeder used was Uniradio 67, a 52 ohm coaxial line with a seven strand, .029 inch copper inner conductor. Since the dielectric constant was not known, preliminary impedance measurements of a fixed short circuited length were made at several frequencies, giving a relative dielectric constant of 2.26. This suggests that the cable was polyethylene filled, an observation substantiated by inspection.

A block diagram of the arrangement and electrical relationship of the components of the system tested is presented as Fig. 8. It is seen that an unspecified frequency indicator forms an inherent part of the system. In an operational system this function would be performed by a form

of discriminator, probably having a D.C. output analogous to the antenna height changes.

For experimental frequency and relative power measurements an Airmec Type 248 Wave Analyser was connected to the loosely coupled probe on the oscillator. The Wave Analyser is a highly selective superheterodyne receiver with both audible and meter output level indications. The latter is calibrated and incorporates adjustable attenuators, so that an output level range of 0-77 decibels is measurable with a sensitivity of plus or minus 1.5 decibels. The receiver is tunable so that by previously calibrating the logging scale, frequencies between 192 and 224 megacycles may be read with an accuracy of plus or minus one logging scale division. This was equivalent to plus or minus 40 kilocycles in the frequency range considered, or readings accurate to the nearest tenth of a megacycle. The logging scale was calibrated against signals from an Airmec Signal Generator. Signals were taken only at the crystal check points on the Signal Generator. These were spaced at eight megacycle intervals in this frequency range. Plotting these frequencies

against logging scale readings on the Wave Analyser produced the linear relation shown in Fig. 9. Hence linear interpolation was assumed possible.

Admittance measurements were made using the General Radio Type 1602 Admittance Meter, an extremely versatile and useful piece of equipment. Fundamentally this meter connects the unknown load in parallel with a 20 millimho standard conductance and a standard susceptance consisting of an adjustable calibrated stub. The use of a stub as a susceptance standard makes the meter's performance independent of frequency. Variable loops couple each of the arms in parallel into a detector arm. The couplings are adjusted until a null is detected, and the positions of the coupling loops are calibrated directly in millimhos admittance. To permit this direct calibration, all the equipment associated with the meter is of 50 ohm characteristic impedance (20 millimhos admittance). This was the reason for choosing the 52 ohm feeder as previously described. Ancillary equipment includes two butterfly type unit oscillators, one used as a generator, the other as

local oscillator in the detector circuit; a crystal detector and 45 megacycle I.F. amplifier (Sanders type I.F.3, serial 003) having meter output level indication. Also several fixed and adjustable 50 ohm air lines and stubs, short and open circuit terminations, and numerous compatible General Radio connectors were provided with the equipment and used in connection with these tests.

In determining the oscillator characteristics a standard, frequency independent, infinitely variable complex load was required. This was obtained by the parallel connection of a standard 20 millimho conductance and an adjustable 20 millimho characteristic admittance short circuited stub, the combination fed by an adjustable section of 20 millimho air line. In terms of load position on the Smith Chart, the locus of the admittance referred to this parallel connection was a circle coincident with the unity normalized conductance circle. Adjustment of the stub produced any desired point on this circle, thereby fixing the standing wave ratio. Adjustment of the feed line length then determined the

phase position of the load on the standing wave circle of constant radius passing through the point set on the first circle. Thus the stub setting determined standing wave ratio, and the line length set the phase of the load, giving in combination any desired value of complex load. This adjustable load connected to the General Radio Admittance Meter is shown in Fig. 10.

The antenna was suspended from a wooden beam constructed by the Works Department of the College. The beam was approximately 14 feet above ground level. Suspension was by means of polyvinyl chloride covered sisal line passing over a fiber pulley. Metallic components were avoided wherever possible in the suspension rig. The suspension line was calibrated directly in inches of the antenna radiating face above the solid earth surface, a calibration which was rechecked at each test to ensure that no line stretch or beam bending had occurred. The only obstacle other than the reflecting earth in the near vicinity was the building wall (clay brick) which was at constant distance from the antenna of 12.5 feet, always greater than the antenna-

ground distance except at the two extreme height points tested. The earth was level packed moist soil with an even growth of grass at a dormant winter height of 1.5 inches. The antenna and support are shown in Fig. 11 viewed from the ground. In Fig. 12 is the supported antenna as seen from above. For one test a group of five bundles of stake fence pickets, each stake measuring about 1.5 inches in diameter and averaging 50.5 inches in height, was placed in the area under the antenna, as shown in Fig. 13, to provide a disruptive reflecting surface. The pickets were joined together by baling wire at one-third and two-thirds their heights to make five discrete bundles when rolled.

EXPERIMENTAL PROCEDURE

Tests were first made on the components alone, the oscillator and the antenna, to determine their individual characteristics. Knowing these, the required length of feeder was then calculated and the system performance as a whole investigated.

Using the previously described variable complex load, the Rieke diagram of the oscillator under several different conditions was obtained. Frequency and relative power under the various conditions of load were measured on the Airmec Wave Analyser. Since the actual value of the load depended on its physical configuration and its frequency, the configuration was noted for each reading and the actual value of the load in conductance and susceptance later determined at the appropriate frequency on the admittance meter. The value of the load was not very sensitive to frequency changes of the order obtained in testing this oscillator. The effect of coupling changes was investigated by obtaining the Rieke diagram as above for three different settings of

the coupling capacitor. The effect of tuning the oscillator was similarly determined by tuning for several different center frequencies (at matched load conditions, $Y = 1 + j0$) and obtaining Rieke diagrams at each. It was decided to operate the oscillator near the minimum anode voltage which would permit stable operation. In this way any adverse effect of low power output could be noted. Further, if it were later desired to use a short length of feeder requiring mounting the oscillator at the antenna and operating it with battery power, low anode voltage would be advantageous. Therefore an anode level of 120 volts was chosen.

With the intention of later comparing this oscillator's performance with that of some commercial product, the Rieke diagram pulling characteristics of one of the General Radio unit oscillators (serial number 1677) were also determined in the same manner.

In testing the antenna, it was first necessary to determine its characteristics in something resembling free space conditions. A wooden floored scaffolding which was in place outside the window in connection with erecting the antenna

support beam was used for this purpose. The antenna was placed on the wooden flooring with its radiating face directed outward and upward from the building and scaffolding. The nearest obstacles were trees and buildings, 30 degrees offset from the normal to the antenna's radiating face and at least 100 yards distant. The antenna admittance was measured at five megacycle intervals from 180 to 240 megacycles using the admittance meter. The total line length, including feeder and adjustable air line was first set to an integral number of half wave lengths as established by repeating a known termination at the meter. In this way the antenna's measured admittance was referred to a point at the cable connector.

Knowing the test oscillator's pulling characteristics from the preceding tests and the range of standing wave ratios which the antenna was able to present from the free space tests, feeder line length calculations were made. The antenna admittance over the ground as a function of height was then measured at three inch intervals and a frequency of 212.5 megacycles. This

frequency corresponded to a VSWR which was expected to give the desirable pulling effect without unstable oscillator operation as determined by the line length calculations. These calculations are presented in Appendix IV.

Minor line length corrections were made to present the desired admittance to the oscillator terminals according to the admittance meter. The amount of standing wave ratio improvement at the input due to line attenuation was noted. The oscillator and antenna were then connected by means of the feeder (and the short length of adjustable line which was allowed for in the calculation). The oscillator was tuned with the antenna at a height of 124 inches, or 2.23λ , giving, according to the earlier tests of admittance, the asymptotic free space admittance in a region where fluctuations due to height change were a minimum. The tests of frequency as a function of height were then conducted, using the Airmec Wave Analyser for frequency indications. These were repeated for verification on separate days, and were made under low wind conditions when antenna motion was the least. Further

similar tests were made at an operating point giving negative $\frac{df}{d\phi}]_{osc}$; at half power output (with reduced anode voltage); over the disruptive reflecting surface (stakes); and with the General Radio oscillator. No peculiarities of the procedure employed were expected to affect the reliability of the results obtained.

RESULTS AND DISCUSSIONS

The behavior of the antenna in "free space" tests in its initially completed form is shown as a curve representing admittance referred to the tap point as a function of frequency on Smith chart coordinates in Fig. 14. Results from which this figure was drawn are presented in Table I. The admittance with reference to the tap point was obtained from that measured with reference to the cable connector by correction for the electrical length of feeder inside the antenna's resonating box between the two points. This was determined experimentally at one frequency. The antenna tap point was short circuited and the admittance at the meter was then measured with an integral number of half wave lengths of feeder inserted between the meter and the cable connector. The electrical length of cable between this admittance and the infinite admittance of the short circuit was next read directly from the Smith chart and corrected proportionately for operation at each of the other frequencies tested.

The antenna performance, according to Fig. 14,

appeared satisfactory for the purposes of this experiment. Operation over a wide range of standing wave ratio within a physically useful frequency bandwidth was observed, including values of VSWR from 0.2 to 0.8 for frequencies between 202 and 234 megacycles.

From inspection of Fig. 14 it was possible to select operating points presenting a range of voltage standing wave ratios to the oscillator. Accordingly a set of representative antenna VSWR's of 0.3, 0.5, and 0.7 was chosen. These were, from Fig. 14, equivalent to operating frequencies of 207, 210, and 212.5 megacycles respectively. The oscillator was tuned to each of these center frequencies in turn with a matched load connected, and the Rieke diagram, or pertinent part thereof, was obtained as previously described. The effect of coupling variation was also examined at the center frequency of 210 megacycles by obtaining the frequency contours of the Rieke diagram at three discrete settings of the coupling capacitor. For all other tests the mid-setting of one turn open was used for this capacitor. Results of the pulling test are listed in Tables II, III, and IV

and presented as Rieke diagrams in Figs. 15, 16, and 17.

The effect of variable coupling, which was considered in the tests to which Fig. 16 applies, was primarily a rotation of the entire diagram due to the effective alteration of line length to the load as more or less capacitance was added. Within the range of capacitance change available the effect of reduced coupling on stability may also be observed. The frequency contours are more widely spaced at lower values of coupling. Power contours and experimental points are omitted from Fig. 16 to improve clarity.

Fig. 17 is drawn on a larger scale Smith chart since, at the frequency considered, only the higher standing wave ratios are possible with the intended antenna load. A comparison of Figs. 15, 16, and 17 shows that tuning this oscillator over the band of frequencies considered has little effect on the shape of the Rieke diagram contours and the oscillator's pulling characteristics.

An analysis of the pulling characteristics in order to determine feeder length and operating point for the complete system was next carried

out. A graph of the form of Fig. 3 was obtained from the information contained in the Rieke diagrams. This graph, appropriate to the center frequencies of Figs. 15, 16, and 17, is presented as Fig. 18. It is seen that the form of the function is the periodic variation of frequency with phase at the oscillator. The amplitude of this function is dependent upon the voltage standing wave ratio. It is apparent that the greater frequency shift is obtained with the smaller VSWR. The shift must not, however, be great enough to permit unstable operation (splitting) with the shortest physically useful cable length. For the case of the VSWR of 0.3, the rate of change of frequency with phase, $\left. \frac{df}{d\phi} \right]_{osc}$, at the oscillator is 5.7 megacycles per radian at the center frequency, limiting the line length to about 5.5 meters. Since it was desired to install the antenna at the end of the support rig provided, and to retain the oscillator on the test bench, this length proved unsatisfactory. The same was true at the operating point where the VSWR was 0.5. Consequently the high frequency operating point was selected.

The chosen point provided an antenna VSWR of 0.7 at a frequency of 212.5 megacycles. The oscillator pulling slope was 2.3 megacycles per radian. The feeder line length appropriate to these conditions was calculated as illustrated in Appendix IV. The exact length of feeder was made subject to alteration by including a section of adjustable air line in the feeder calculations. This permitted adjustment of the operating conditions at will.

Antenna admittance over the ground at the chosen operating frequency was next investigated. Since the use intended for this phenomenon was the pulling of the oscillator, it was decided to refer this admittance to the oscillator output connector. This was expected to permit direct correlation with the frequency-height relation to be obtained later. Furthermore, comparison between these tests and the oscillator Rieke diagrams was possible, since both were referred to the same datum. This datum was established in the equipment by adjusting the feeder length to obtain the desired operating admittance shown in Fig. 17 at the generator end with the antenna

in free space conditions.

The results of the admittance measurements over the ground are indicated in Table V and plotted in conductive and susceptive components in Fig. 19. From this plot the graph of Fig. 20 showing the same relationship on Smith chart coordinates was constructed.

A comparison of Figs. 2 and 19 shows that the result predicted by theory for a thin half wave dipole over a plane reflecting surface was closely realized in the case of this practical directive antenna over the real earth. Similar admittance-height functions, periodic with quarter wave length intervals, and having decreasing amplitudes with height, apply to both cases. It was therefore concluded that the experimental arrangements were sufficiently free from spurious effects to permit a meaningful test of the expected frequency-height relationship.

This work completed the examination of the performance of each of the components which were to make up the system. No significant deviations from the expected characteristics had been observed. The remainder of the experimentation

dealt, therefore, with tests of the operation and performance of the assembled system. It should be stated at this point that the term "system" refers only to the skeleton laboratory arrangements made for examining the validity of this approach to low height determination. In particular the oscillator employed was in no sense capable of operational installation. Further, the reading of frequency was done on bulky laboratory equipment, omitting the desirable step of employing a discriminator to produce a more useful D.C. output as a height change analog.

The equipment was first connected to produce operation at the desired frequency and load impedance, as described in the Procedure section. The VSWR at the oscillator was somewhat better than that predicted by the antenna characteristics in Fig. 14 because of line attenuation. This improvement in VSWR made the oscillator slightly more stable and could have been used to permit a longer feeder installation if necessary. It was felt that the change was small enough to leave the pulling characteristic substantially unaffected.

The readings obtained for frequency as a function of height in this configuration and in others described below are presented in Table VI. Fig. 21 indicates graphically the result obtained in this primary operating configuration. The expected result was obtained, in that a periodic deviation of frequency about the center tuned value occurred. The amplitude of the swing decreased with height, approaching the center tuned frequency, corresponding to free space conditions, asymptotically.

It is of interest to compare the observed height-frequency relation with the height-admittance relation measured on the antenna alone. The relevant figures are Figs. 19 and 21. It is seen that the susceptible part of admittance changes and the height-frequency curve correspond directly in periodicity and zero deviation heights (from free space and center frequency conditions). A comparison of Figs. 17 and 20 indicates more clearly the reason for this correspondence. The maximum pulling of frequency occurs at those heights corresponding to the greatest phase angle displacement of the admittance spiral from the

oscillator's center frequency contour. Zero frequency deviation occurs for coincidence of the admittance spiral and the center frequency contour. In this particular case the frequency contours and susceptance lines on the Smith chart are nearly parallel in the operating region. The conductance lines are nearly orthogonal to the frequency contours. Therefore the susceptance-height and frequency-height relations coincide when the former is referred to the oscillator terminals. The conductance-height relation is, as seen in Fig. 19, nearly 90 degrees out of phase with the frequency-height curve of Fig. 21. In general it is neither input conductance nor input susceptance which determines the frequency-height relation. It is antenna input admittance taken as a whole and, in particular, that generally undefined component of admittance referred to the oscillator and having changes perpendicular to the pulling contours which determines the frequency changes corresponding to height.

It is felt that results are less valid near the top of the test range due to relative proximity of the building. The function passed

through center frequency at approximately quarter wave length intervals above the ground. The shape of the function was dictated largely by the pulling characteristic of the oscillator. It was by no means sinusoidal because of the concavity of the oscillator frequency contours toward the low frequency side of the center value. Thus the output of such a system appears to be more useful (possibly exclusively useful) at the center frequency points. Whether these occur at small enough intervals to provide a reasonable data rate depends upon the desired application. The above results were found to be repeatable on different days to within the accuracy of plotting the data in the form of Fig. 21.

In order to obtain a high-low indication of predetermined sense from a characteristic such as Fig. 21, it would be possible to consider only alternate center frequency points. In such a case a particular sense of frequency deviation would have a particular sense of height deviation. It is of interest to consider the height errors produced by the experimental system examined here for the several center frequency points

encountered. Table VII presents this information. For a set of center frequencies corresponding to positive-going "on height" frequency readings, the magnitude and percentage errors are given in columns 2, 3, and 4. The lowest height of the set corresponding to center frequency is taken as correct because, having the greatest frequency swing, it presents the least probable height uncertainty. Similarly, columns 5, 6, and 7 present the same information for a set of negative-going "on height" center frequencies.

Tests of the frequency-height relationship were made in several different operating conditions. A fifty per cent reduction in power output was made by lowering the anode voltage of the oscillator until the Wave Analyser indicated three decibels less relative power. The result is presented in Fig. 22. The general shape of the function remains as in Fig. 21 with an amplitude of swing only very slightly less. Center frequency points are altered by less than 0.02 wave lengths. The Rieke diagram of the oscillator at the new anode voltage was examined and found to have small changes in shape compared with Fig. 17.

The slight differences in this characteristic account for the small changes in center frequency which are present in Fig. 22. In general the equipment seemed relatively insensitive to small power changes because of the above results obtained at a power change of fifty per cent and the repeatability of all tests performed.

The system was reset to operate at an oscillator-referred load admittance diametrically opposite in Fig. 17 to that of the first test. In this condition the value of $\left. \frac{df}{d\phi} \right|_{osc}$ was approximately the negative of that normally chosen. Stability of operation remains the same, but the effect of electrical feeder length change is to oppose the phase change due to the antenna admittance varying with height over the ground. The result of the test was as shown in Fig. 23. Power output was the same as for normal operation in Fig. 21. A comparison indicates that the expected reduced pulling occurred. The desirability of selecting an operating point in which the feeder length effect is utilized is thus shown.

The final test of the experimental system was made over a disruptive reflecting surface

consisting of five bundles of wooden fence stakes of various cut lengths averaging about 50.5 inches. The result is presented as Fig. 24. It may be described as a repeat of Fig. 21 but with a zero height level at a virtual height of 49.9 inches (0.9 wave lengths) indicating that the stakes appeared as nearly a plane reflector. The shape of the function appears markedly more like a damped sinusoid than does that of Fig. 21. This suggests that propagation considerations in this instance may have balanced the irregularity introduced by the oscillator pulling characteristic shape.

As a further consideration it was desired to demonstrate the significance of the oscillator pulling characteristic in the operation of the system. One of the General Radio butterfly type unit oscillators was tested at a particular setting of its variable coupling loop. The Rieke diagram obtained is shown in Fig. 25. Operation in the vicinity of the convergence of frequency contours was difficult, and the choice of that region for system operation was felt to be unwise due to instability and low power output. In

other parts of the diagram the oscillator was seen to be less susceptible to pulling than the experimental line oscillator used in this thesis. Frequency-height tests were made at positive slope operating points as indicated in Fig. 25 (VSWR of 0.2, 0.3) where the greatest value of $\left. \frac{df}{d\phi} \right|_{osc}$ possible was anticipated. No readable frequency change was obtained over the entire height range from 0.2 to 2.3 wave lengths. The importance of having an oscillator with fairly closely spaced frequency contours (the result of tight load coupling) is indicated.

SYSTEM REALIZATION AND APPLICATION

As a result of the tests and analysis performed in this approach to low height determination, certain statements may be made regarding the practical realization of such a system.

An early consideration in system design is the choice of frequency. The amount of reflected energy returned to the antenna relative to the amount which is radiated appears to limit the useful height range of the system. Within such a height envelope, the number of useful center frequency points varies directly with the frequency of operation, since these occur at quarter wave length intervals. Center frequency "on height" points do not define specific heights; hence they are ambiguous without further refinements. Procedures such as counting down from some known point determined by another height sensing input, or correlating the amplitude of the frequency shift to the known frequency-height function of the system are possible methods of resolving the ambiguity. The advantage of simplicity may be lost if such methods are employed.

Consequently some frequency compromise will be required which will give a sufficient number of "on height" points without introducing excessive ambiguity. The intended application, including required accuracy and flight path, will dictate this choice.

Oscillator design should be the next consideration. The primary feature should be closely spaced frequency contours on the Rieke diagram so that the oscillator can be pulled readily. Adjustable coupling to the load is a good method of achieving flexibility at this stage, since the coupling is important in determining the spacing of the frequency contours. The power output of the oscillator should be fairly constant for a wide range of loads to permit more efficient operation, although this characteristic is not critical. Loose coupling to the indicating equipment should be provided so that the oscillator will not be loaded from this direction.

Having designed an oscillator which can be pulled by an amount suitable for discrimination, with fairly constant power output at high values of VSWR, the antenna and installation may be

considered. The desirable features of this are good directivity in the downward direction and a VSWR at the operating frequency of the order of 0.7 or better. The latter may have to be reduced if the oscillator's pulling slope, $\left. \frac{df}{d\phi} \right]_{osc}$, is too small. The entire system will operate more efficiently if the VSWR is kept high.

The feeder, which is the most flexible item from a designer's point of view, is determined last. The fractional half wave length portion of feeder is that length needed for matching the antenna and oscillator admittances at the desired frequency. The integral number of half wave lengths of feeder are determined by the limiting length for stable oscillation without splitting. How closely this unstable limit is approached will depend upon the need for magnifying the antenna admittance changes over ground to pull the oscillator adequately. In most cases the maximum allowable feeder effect will be desirable. If installation limitations dictate a very short feeder, the augmenting of this by a suitable phase shifting lumped parameter network at the appropriate frequency may be considered. For

simplicity and reliability it might be more satisfactory to install some physically redundant cable if possible.

The final required component would be the discriminating-indicating device. A prime requirement would be a low input power requirement, permitting loose coupling to the oscillator. The probable desired discriminator characteristic would be zero output for center frequency operation of the oscillator with a positive D.C. output proportional to frequency deviations in one sense and a negative D.C. output proportional to frequency deviations in the opposite sense. Being determined by the oscillator frequency, the discriminator's output would therefore be analogous to the vehicle's height condition. Any of the discriminators commonly employed in radar applications might be considered. The choice of resonant cavity methods of frequency comparison as in Pound discriminators or tuned lumped circuit comparison as in Weiss discriminators may be dictated by the operating frequency selected. The design and testing of a suitable discriminator were not within the intended scope of this thesis.

CONCLUSIONS

If the radio frequency energy of an oscillator is radiated from an antenna and directed toward a reflecting surface, it has been shown that the oscillator's frequency may be related to the distance between the antenna and the surface; providing that distance is not too great. This is the most important result of these investigations. The relationship observed is a periodic variation of frequency with height about a center tuned frequency. Zero deviation from the center frequency occurs at quarter wave length height intervals above ground and the magnitude of the deviation decreases with increasing height. The center frequency is approached asymptotically, but the effect is expected to be of little use above the height range tested. It has been established experimentally that the above result, held initially to be theoretically possible, is a primary effect when the distance involved is small enough for significant antenna admittance changes to occur.

In establishing this result it has been

observed that periodic changes in the real and imaginary parts of antenna admittance take place as a function of separation between the antenna and a reflecting surface. The quality and character of reflection has been shown to be non-critical for this effect, providing sufficient energy is returned to the antenna. That is, the nature of the function relating admittance to height appears relatively independent of the reflecting surface. A direct correspondence was observed between the height-frequency relation of the first conclusion and the imaginary (susceptive) part of the height-admittance relation when referred to the oscillator terminals.

The feeder cable employed in connecting the oscillator and antenna may be used as a phase shifting device, effectively magnifying any phase changes occurring at the antenna. This effect is dependent on the length of cable and on the admittance match achieved between the antenna and oscillator.

An oscillator delivering energy to a load has its frequency and power output partially determined by that load (including the means of coupling), as

well as by the oscillating circuit parameters themselves. This effect, established at the outset by theoretical considerations, has been shown experimentally to be of practical value in obtaining a predictable relationship between antenna admittance and oscillator frequency.

ACKNOWLEDGEMENTS

It is the author's desire to indicate clearly that Mr. R. Thomason was the source of the ideas for the system of height determination considered in this thesis. As the member of the College staff responsible for counseling and guidance in connection with this project, Mr. Thomason was always ready to provide assistance of the highest quality. His kindness and encouragement are gratefully appreciated.

The prompt and efficient service of Mr. Pollard and his staff in the College Works Department in connection with constructing a highly serviceable test rig, mounting the antenna, and machining the tuned lines is acknowledged with thanks.

REFERENCES

- Ref. 1: Hansford, R.F.: Radio Aids to Civil Aviation, Sec. 4.23; Appendix B, Sec. 1.2.1; 1960, 1st ed., T. & A. Constable Ltd., Edinburgh.
- Ref. 2: Jordan, E.C.: Electromagnetic Waves and Radiating Systems, Sec. 12.08, 1953, 1st English printing, Constable & Co., Ltd., London.
- Ref. 3: Reintjes, J.F. and Coate, G.T.: Principles of Radar, Chap. X Art. 10, 1953, 3rd ed., McGraw-Hill Publishing Co. Inc., New York.
- Ref. 4: Thomason, R.: A Proposed System for an Automatic Height Lock, Appendix 1, 6 June 1961, Internal Technical Memo No. 3, Department of Electrical and Control Engineering, The College of Aeronautics, Cranfield, England.
- Ref. 5: Schelkunoff, S.A., and Friis, H.T.: Antennas Theory and Practice, Secs. 9.7, 9.8, 13.3, 13.4, 13.5, 1952, 1st ed., John Wiley & Sons, Inc., New York.

- Ref. 6: Carter, P.S.: Circuit Relations in Radiating Systems and Applications to Antenna Problems, Proceedings of the Institute of Radio Engineers, June 1932, Vol. 20, pp. 1004-1041.
- Ref. 7: Smith R.A.: Aerials for Metre and Decimetre Wave Lengths, Chap. 2, Table 3, Art. 2.7, 1949, 1st ed., Cambridge University Press, Cambridge.
- Ref. 8: Jordan, E.C.: Electromagnetic Waves and Radiating Systems, Sec. 8.08, 1953, 1st English printing, Constable & Co. Ltd., London.

APPENDIX I

INPUT ADMITTANCE OF THE HALF WAVE DIPOLE OVER A PLANE REFLECTING SURFACE

The antenna and reflecting surface may, as explained in the body of the report, be considered as an antenna and its image in free space. Such a system is a two-port network in which the feed point of the antenna is port 1 and the feed point of the image is port 2. The theory of linear two-ports may be applied (Ref. 5):

$$e_1 = z_{11}i_1 + z_{12}i_2 \quad (3)$$

$$e_2 = z_{21}i_1 + z_{22}i_2 \quad (4)$$

$$i_1 = y_{11}e_1 + y_{12}e_2 \quad (5)$$

$$i_2 = y_{21}e_1 + y_{22}e_2 \quad (6)$$

The subscripts 1 and 2 refer to the respective ports. In this case of passive elements, reciprocity applies giving

$$z_{12} = z_{21} ; y_{12} = y_{21} \quad (7)$$

The requirement for zero tangential electric vector at the reflecting surface is met if

$$i_2 = -i_1 \quad (8)$$

and

$$e_2 = -e_1 \quad (9)$$

Under these conditions (3) and (5) may be solved to obtain the input admittance and impedance of the antenna:

$$z \equiv \frac{e_1}{i_1} = z_{11} - z_{12} \quad (10)$$

$$y \equiv \frac{i_1}{e_1} = y_{11} - y_{12} \quad (11)$$

The mutual impedance coefficient, z_{12} , has been calculated (Refs. 6 and 7) for various separations of antenna and image up to three wave lengths. The calculations are made on the assumption of sinusoidal current distribution, which is valid for infinitely thin half wave antennas, in which second and higher order mutual effects do not occur.

The self impedance coefficient, z_{11} , is the limit of z_{12} as the separation tends to zero, so that the input impedance, z , is zero with the antenna on the ground. The value of z_{11} is $73.3 + j42.2$ ohms.

To obtain y_{12} from z_{12} , the linear two-port equations (3) through (6) may be combined to give:

$$y_{12} = \frac{-z_{12}}{z_{11}z_{22} - z_{12}z_{21}} \quad (12)$$

In this case since $z_{21} = z_{12}$ by reciprocity, and

$z_{22} = z_{11}$ by symmetry:

$$y_{12} = \frac{-z_{12}}{z_{11}^2 - z_{12}^2} \quad (13)$$

or in terms of real and imaginary components:

$$g_{12} = - \frac{r_{12}(r_1^2 + x_{12}^2 - r_{12}^2 - x_1^2) + x_{12}(2r_1x_1 - 2r_{12}x_{12})}{(r_1^2 + x_{12}^2 - r_{12}^2 - x_1^2)^2 + (2r_1x_1 - 2r_{12}x_{12})^2} \quad (14)$$

$$b_{12} = - \frac{r_{12}(2r_{12}x_{12} - 2r_1x_1) + x_{12}(r_1^2 + x_{12}^2 - r_{12}^2 - x_1^2)}{(r_1^2 + x_{12}^2 - r_{12}^2 - x_1^2)^2 + (2r_1x_1 - 2r_{12}x_{12})^2} \quad (15)$$

The reciprocal of z_{11} taken directly yields y_{11} ,

the self impedance of this ideal antenna, as

10.25-j5.90 millimhos.

Values of input admittance, y , were calculated according to equations (11), (14), and (15) from the values of mutual impedance obtained from the literature to which reference has been made. The range of heights considered began at 0.15λ since experimental measurements were not made below that height. At lower heights the antenna theories applied become less valid because of

the increasing importance of radial field components. These vary as the inverse square of distance from the antenna and are therefore usually ignored beyond distances of the order of one-fourth wave length. The transverse radiation fields on which antenna theory is developed vary inversely with distance and are predominant at distances greater than about one-sixth of a wave length. Mutual impedances for heights greater than 1.5 wave lengths were not obtained. It is felt that this range of heights is sufficient to show the nature of the theoretical admittance-height relationship. The results of these computations of input admittance are presented as Fig. 2.

APPENDIX II

THE EFFECT OF LOAD ON OSCILLATOR FREQUENCY

The oscillator with coupled load may be regarded as a simple RLC parallel resonating circuit with a load, having resistive and reactive components, connected across it. The resonating circuit represents the more complicated combination of components producing resonant oscillations in the tuned line push-pull oscillator with artificially introduced feedback used in these tests. The load in this case is the equivalent of the varying complex impedance of the antenna, the phase shift and attenuation of the feeder cable, and the coupling capacitor used to connect the load to the oscillating circuit. Thus the reactive component of load will consist of capacitance and may have inductance as well, depending upon the chosen line length, height of the antenna above ground, and the frequency of oscillation. Fig. 26a is a diagram of the arrangement described. Fig. 26b is the equivalent combination of parallel load components. The reactive branch of the load, $X_L \left[1 + \left(\frac{R_L}{X_L} \right)^2 \right]$, is

seen in Fig. 26b to form, with the L and C branches, a third frequency dependent branch of the resonator. Thus the oscillating frequency depends on the values of all the components of the load, both resistive and reactive. The

equivalent load resistance, $R_L \left[1 + \left(\frac{X_L}{R_L} \right)^2 \right]$, also

depends on all the components of the load. Therefore the power output which depends on the resistive part of the equivalent load, is determined by the particular combination of load and coupling chosen.

In the case of a high frequency oscillator, where many different load variables affect the power output and frequency, it is useful and convenient to depict the output characteristics of the oscillator in the form of a Rieke diagram for representative conditions of the controllable load variables. This approach permits the logical separation of the effects of controlled and uncontrolled load conditions. The latter are allowed to vary over their entire range for each diagram which represents a fixed setting of the controlled conditions, such as coupling, line length, and

setting of tuning controls.

The Rieke diagram consists of lines or contours of constant frequency and of constant power output as functions of load, usually drawn on Smith chart coordinates. The desirable feature is that such contours be without intersections so that continuous changes of load will produce continuous changes of frequency. In order for each value of complex load to permit oscillation at a single frequency, the total susceptance of the equivalent circuit of Fig. 26b must be zero at only one frequency for each value of load conductance and susceptance imposed. The susceptance of the entire equivalent load branch is

$$\frac{1}{X_L \left[1 + \left(\frac{R_L}{X_L} \right)^2 \right]} = \frac{X_L}{X_L^2 + R_L^2} \quad (16)$$

which is proportional to X_L times a positive number, and so must pass from negative to positive values through resonance with increasing frequency. The oscillator branches L and C combine in parallel to produce a net susceptance passing from positive to negative values through resonance. If the oscillator and load susceptances combined are to be zero at a single resonant frequency, the

load susceptance must be kept relatively small in the neighborhood of resonance, whether or not their separate resonant frequencies are exactly identical. Inspection of (16) indicates that this will be the case if R_L is kept sufficiently large and the coupling and reactive components of the load are sufficiently small. The magnitudes which are sufficient depend on the sharpness of resonance of the oscillator tuned circuit. Critical combinations of the load parameters which would result in large contributions of load susceptance at frequencies just off oscillator resonance must be avoided.

APPENDIX III

OSCILLATOR DESIGN CALCULATIONS

1. Anode Lines

a. Length and tuning

Specified output capacity of tube: 1.6 pf.

For zero adjustable capacitance added, a frequency of 215 megacycles results in capacitive reactance of 463 ohms. The corresponding line length to resonate with this by producing an equal inductive reactance depends on the short-circuited transmission line formula:

$$X_L = Z_L = Z_0 \tan \frac{2\pi l}{\lambda} \quad (17)$$

The characteristic impedance of the intended rectangular cross section transmission lines of depth to spacing ratio of unity was determined from published transmission line data to be 180 ohms. Solving (17) for l at resonance at 215 megacycles gave

$$l = 0.267 \text{ meters.} \quad (18)$$

To tune for a lower frequency it was arranged to introduce a parallel capacitive disc with a circular area one-half inch in diameter and minimum practical spacing from

the opposite conductor of $\frac{1}{32}$ inch. For dimensions in inches:

$$C = .224 \frac{A}{d} \times 10^{-12}, \quad (20)$$

or a maximum adjustable capacitance of 1.4 pf.

The 26.7 centimeter line has a reactance of 292 ohms at 181 megacycles by (17). Since the total capacitance of 3.0 pf. has an equal and opposite reactance at this frequency, 181 megacycles is the lowest tunable frequency for this line and capacitor combination.

b. Quality factor Q

The quality factor is given by (Ref. 8)

$$Q = \frac{\pi}{\lambda \alpha} \quad (21)$$

where $\alpha \approx \frac{R}{2Z_0}$, R in this case being resistance per unit length of line. Taking the material to be copper and a depth of $\frac{1}{4}$ inch in the formula for resistance

$$R = \frac{1}{a} R_{\text{surface}} = \frac{1}{a} \sqrt{\frac{\pi f \mu}{\sigma}} \quad (22)$$

gives $R = 0.582$ ohms per meter and $Q = 1295$ in (21) at 200 megacycles.

2. Grid Lines

a. Length and tuning

Specified input capacity of tube: 4.4 pf.

With line of depth $\frac{1}{2}$ inch and depth to spacing ratio of 0.5, published data gives $z_0 = 250$ ohms. Such a short circuited line will resonate at 215 megacycles with the specified input capacitance if, by (17), it is 13.3 centimeters long.

An adjustable circular disc capacitor similar to that in part 1 will give a maximum total capacitance on the tube input side of 5.8 pf. The corresponding resonant frequency for a 13.3 centimeter line is 189 megacycles, giving the tuning range of the grid lines as 189 to 215 megacycles.

b. Quality factor Q

By (22) R for the grid lines is 0.291 ohms per meter. By (21) the corresponding Q is 3590 at 200 megacycles.

APPENDIX IV

FEEDER LENGTH CALCULATIONS

As an illustration, the calculation procedure for positive pulling slope operation at 212.5 megacycles is explained. The reciprocal rate of change of phase on the cable with frequency is inversely proportional to cable length. From (2):

$$\left[\frac{df}{d\phi} \right]_{\text{line}} = \frac{c_{\text{cable}}}{2\pi l} \quad . \quad (23)$$

This quantity must be at least as large as the corresponding rate of change of frequency of the oscillator with load phase presented, to allow stable oscillator operation as discussed under Theory. The measured oscillator pulling rate from Fig. 18 is 2.3 megacycles per radian. Therefore:

$$1 \leq \frac{c_{\text{cable}}}{4.6 \pi \times 10^6} \quad . \quad (24)$$

Since

$$\sqrt{\epsilon_r} c_{\text{cable}} = c_{\text{air}} \quad , \quad (25)$$

for Uniradio 67 cable $c = 1.98 \times 10^8$ meters per second. The limiting length is, by (24), 13.7

meters. Within this length, an integral number of half wave lengths plus a fractional half wave length sufficient to match antenna and oscillator load impedance must be included.

As a practical consideration, a length of adjustable air line was also included to permit precise adjustment of the antenna-oscillator match. The cable was actually cut to 30 feet (9.16 meters) to permit tests at other, less stable, oscillator operating conditions, and to provide a conservative margin of design flexibility at the desired operating point.

TABLE I

Antenna Admittance in Free Space

Date of Test: 5th December 1961

f	G	B	Correction
megacycles			fractional λ c
180	+ 0.69	+2.60	0.130
185	11.9	-1.30	0.134
190	6.10	-4.82	0.138
195	1.56	-3.02	0.141
200	0.68	-1.60	0.145
205	0.47	-0.89	0.148
210	0.55	-0.30	0.152
215	0.92	+0.19	0.156
220	1.85	-0.12	0.159
225	1.38	-1.23	0.163
230	0.52	-1.03	0.167
235	0.31	-0.73	0.170
240	0.19	-0.43	0.174

Note! Measurements are referred to antenna panel connector.

Corrections applied "toward load" to obtain reference to antenna tap point.

TABLE II.

Oscillator Rieke Diagram

Date of Test: 28th January 1962.

Center Frequency: 207 megacycles
Anode Voltage: 120 V. Coupling: Medium (One turn)

f	stub length	line extension	relative power	G	B
megacycles	cm	cm	dB		
204	14.6	68.8	- 6.0	+3.28	+0.04
204	14.6	70.8	-15.0	3.16	-0.92
205	14.6	62.5	- 1.5	2.22	+1.45
205	18.0	62.2	- 2.0	2.14	0.72
205	18.0	71.3	-11.5	1.99	-0.91
206	14.6	56.4	- 0.5	1.04	+1.34
206	18.0	73.2	-10.5	1.60	-1.06
206	18.0	55.0	- 0.5	1.25	+1.03
206	21.4	55.9	- 1.5	1.45	0.69
206	21.4	70.0	- 6.5	1.66	-0.62
206	24.5	65.0	- 3.5	1.63	-0.18
206	24.5	61.1	- 3.5	1.65	+0.14
207	14.6	3.0	-14.0	1.40	-1.53
207	14.6	50.8	- 0.5	0.69	+1.03
207	18.0	48.7	- 1.0	0.80	0.83
207	18.0	3.8	- 7.0	1.18	-1.05
207	21.4	49.3	0	1.03	+0.70
207	24.5	47.1	- 1.5	1.02	0.51
207	24.5	0.0	- 5.5	1.30	-0.53
207	27.8	42.6	- 0.5	0.95	+0.30
207	30.4	35.0	- 2.5	0.88	0.15
207	30.4	3.1	- 2.0	1.05	-0.22
207	35.5	9.1	0	1.01	+0.03

TABLE II (Cont.)

f	stub	line	relative		
megacycles	length	extension	power	G	B
	cm	cm	dB		
208	14.6	4.6	-7.5	+1.11	-1.38
208	14.6	45.4	-1.0	0.47	+0.71
208	18.0	42.1	-1.0	0.55	0.55
208	18.0	8.0	-4.5	0.82	-0.83
208	21.4	6.7	-4.0	0.92	-0.65
208	21.4	40.0	+1.5	0.65	+0.44
208	24.5	36.2	+1.0	0.69	0.30
208	24.5	9.1	-3.5	0.84	-0.43
208	27.8	24.3	-0.5	0.71	0
209	14.6	7.5	-5.0	0.77	-1.13
209	14.6	38.5	-2.0	0.28	+0.47
209	18.0	35.5	-0.5	0.44	0.30
209	18.0	20.0	-3.5	0.43	-0.28
209	21.4	23.5	+0.5	0.51	-0.08
209	21.4	21.5	0	0.52	-0.15
210	14.6	11.9	-4.0	0.54	-0.77
210	14.6	32.3	-2.0	0.31	+0.15

TABLE III

Oscillator Rieke Diagram

Date of Test: 7th February 1962

Center Frequency: 210 megacycles. Anode Voltage: 120 V.

(1) Loose Coupling				
f	stub length	line extension	G	B
megacycles	cm	cm		
207	11.0	2.4	+1.68	-2.18
207	14.6	2.2	1.42	-1.50
208	11.0	0	2.70	-2.38
208	14.6	70.5	2.18	-1.51
208	18.0	70.6	1.69	-1.04
209	11.0	69.0	4.35	-1.56
209	14.6	66.3	3.38	-0.42
209	18.0	65.5	2.43	-0.44
209	21.4	65.3	1.89	-0.38
209	24.5	76.8	0.94	-0.51
210	11.0	65.8	4.55	+1.30
210	14.6	62.6	2.93	1 .10
210	18.0	60.4	2.33	0.67
210	21.4	58.4	1.83	0.47
210	24.5	59.1	1.68	0.10
211	11.0	62.4	2.42	2.38
211	14.6	58.2	1.73	1.54
211	18.0	54.9	1.43	1.10
211	21.4	50.9	1.19	0.75
212	11.0	57.3	0.97	1.75
212	14.6	51.6	0.78	1.14
212	18.0	49.6	0.89	0.92
212	21.4	44.1	0.79	0.60
212	24.5	39.3	0.77	0.42

TABLE III (Cont.)

(ii) Medium Coupling				
f	stub length	line extension	G	B
megacycles	cm	cm		
207	11.0	15.2	+0.35	-0.81
207	14.6	13.3	0.48	-0.73
207	18.0	14.2	0.54	-0.54
208	11.0	13.4	0.40	-0.93
208	14.6	11.0	0.57	-0.87
208	18.0	10.2	0.67	-0.72
208	21.4	10.9	0.72	-0.52
209	11.0	11.6	0.47	-1.07
209	14.6	8.5	0.71	-1.06
209	18.0	6.6	0.87	-0.89
209	21.4	5.1	0.98	-0.68
209	24.5	5.7	0.92	-0.50
210	11.0	9.7	0.56	-1.25
210	14.6	6.0	0.89	-1.22
210	18.0	3.0	1.18	-1.02
210	21.4	0	1.36	-0.73
210	24.5	70.5	1.27	-0.53
211	11.0	7.5	0.75	-1.50
211	14.6	3.2	1.25	-1.43
211	18.0	70.3	1.77	-1.02
211	21.4	66.7	1.79	-0.51
211	24.5	63.7	1.64	-0.24
212	11.0	5.2	1.04	-1.78
212	14.6	69.8	2.39	-1.44
212	18.0	64.8	2.50	-0.28
212	21.4	59.1	1.89	+0.38

TABLE III (Cont.)

(iii) Tight Coupling				
f	stub length	line extension	G	B
megacycles	cm	cm		
207	11.0	15.6	+0.34	-0.78
207	14.6	14.1	0.46	-0.68
207	18.0	16.5	0.49	-0.44
208	11.0	14.1	0.38	-0.88
208	14.6	11.6	0.55	-0.84
208	18.0	11.5	0.63	-0.67
209	11.0	12.1	0.45	-1.04
209	14.6	9.3	0.66	-0.99
209	18.0	7.8	0.80	-0.84
209	21.4	7.2	0.87	-0.64
209	24.5	9.0	0.80	-0.43
210	11.0	10.3	0.53	-1.20
210	14.6	7.0	0.82	-1.16
210	21.4	2.0	1.19	-0.74
210	24.5	1.0	1.16	-0.53
211	11.0	8.3	0.68	-1.40
211	14.6	4.3	1.10	-1.35
211	18.0	0.2	1.55	-1.06
211	21.4	68.7	1.62	-0.63
211	24.5	65.7	1.55	-0.37
212	14.6	71.7	1.83	-1.56
212	21.4	62.3	1.98	-0.03
212	24.5	57.8	1.65	+0.22

TABLE IV

Oscillator Rieke Diagram

Date of Test: 14th February 1962.

Center Frequency: 212.5 megacycles
Anode Voltage: 120 V. Coupling Medium: (One turn)

f	stub length	line extension	relative power	G	B
megacycles	cm	cm	dB		
211	24.5	15.4	-10.0	+0.67	-0.22
211	24.5	5.5	- 3.0	0.93	-0.44
211.5	24.5	18.4	- 9.0	0.64	-0.14
211.5	24.5	71.3	- 1.0	1.13	-0.51
211.5	27.8	7.5	- 6.0	0.89	-0.27
211.5	27.8	3.2	- 3.0	1.01	-0.30
212	24.5	21.5	- 7.0	0.63	-0.05
212	24.5	67.1	- 1.0	1.36	-0.45
212	27.8	17.8	- 6.0	0.75	-0.09
212	27.8	66.0	- 1.0	1.22	-0.26
212	30.4	17.0	- 4.0	0.86	-0.04
212	30.4	65.2	- 1.0	1.14	-0.15
212.5	24.5	24.8	- 6.0	0.62	+0.04
212.5	24.5	63.4	- 1.0	1.53	-0.31
212.5	27.8	24.0	- 5.0	0.74	+0.03
212.5	27.8	58.9	- 1.0	1.36	-0.04
212.5	30.4	26.6	- 3.0	0.85	+0.09
212.5	30.4	55.3	- 2.0	1.20	0.00
213	24.5	28.9	- 5.0	0.64	0.15
213	24.5	57.9	- 1.0	1.60	0.06
213	27.8	30.0	- 4.0	0.78	0.15
213	27.8	50.1	- 2.0	1.23	0.24
213.5	24.5	37.0	- 3.0	0.75	0.36
213.5	24.5	52.4	- 2.0	1.42	0.38

TABLE V

Antenna Admittance over Ground

Date of Test: 2nd March 1962

Generator Frequency: 212.5 megacycles

h inches	h/λ	G	B	h inches	h/λ	G	B
10	0.18	+0.600	0	73	1.31	+0.835	+0.170
13	0.23	0.625	+0.140	76	1.37	0.855	0.175
16	0.29	0.700	0.250	79	1.42	0.915	0.175
19	0.34	0.800	0.330	82	1.48	0.935	0.140
22	0.40	0.990	0.350	85	1.53	0.940	0.110
25	0.45	1.152	0.198	88	1.58	0.915	0.075
28	0.50	1.110	0	91	1.64	0.860	0.070
31	0.56	0.940	-0.050	94	1.69	0.855	0.080
34	0.61	0.840	-0.010	97	1.74	0.830	0.090
37	0.66	0.800	+0.050	100	1.80	0.840	0.105
40	0.72	0.785	0.110	103	1.85	0.840	0.115
43	0.77	0.800	0.150	106	1.91	0.850	0.125
46	0.83	0.830	0.185	109	1.96	0.865	0.115
49	0.88	0.885	0.200	112	2.02	0.885	0.110
52	0.94	0.945	0.190	115	2.07	0.860	0.085
55	0.99	0.985	0.120	118	2.12	0.850	0.080
58	1.04	0.940	0.050	121	2.18	0.840	0.095
61	1.10	0.860	0.045	124	2.23	0.835	0.105
64	1.15	0.830	0.065	127	2.28	0.840	0.115
67	1.20	0.810	0.100	130	2.34	0.860	0.130
70	1.26	0.810	0.140				

Note! Admittances are referred to oscillator output terminals for 212.5 megacycles operation.

TABLE VI

System Performance - Frequency as a Function of Height

Date of: Test 1, Normal Operation, 2nd March 1962
 Test 2, Half Power, 22nd March 1962
 Test 3, Negative Slope, 6th March 1962
 Test 4, Disruptive Surface, 12th March 1962

Test No.		1	2	3	4
h inches	h_{λ}	f mc/s	f mc/s	f mc/s	f mc/s
10	0.180	210.48	210.74	213.28	
13	0.234	212.98	210.48	213.03	
16	0.288	213.36	212.98	212.82	
19	0.342	213.40	213.23	212.60	
22	0.396	213.19	213.28	212.39	
25	0.450	212.48	213.14	212.18	
28	0.505	212.48	212.90	212.27	
31	0.558	211.93	212.52	212.64	
34	0.612	211.29	212.05	212.77	
37	0.667	210.96	211.58	212.82	
40	0.722	211.29	211.04	212.77	
43	0.775	212.68	212.35	212.73	
46	0.828	212.90	212.68	212.60	
49	0.883	212.90	212.82	212.52	
52	0.938	212.82	212.86	212.48	
55	0.991	212.60	212.77	212.43	
58	1.045	212.31	212.56	212.56	210.78
61	1.100	211.97	212.18	212.68	209.00
64	1.155	211.37	211.84	212.73	213.53
67	1.210	212.27	212.01	212.73	213.57
70	1.260	212.56	212.43	212.68	213.53
73	1.315	212.77	212.64	212.60	213.40
76	1.370	212.82	212.73	212.56	213.03
79	1.425	212.86	212.77	212.48	212.73

TABLE VI (Cont.)

Test No.		1	2	3	4
h inches	h_{λ}	f mc/s	f mc/s	f mc/s	f mc/s
82	1.480	212.73	212.68	212.48	212.56
85	1.530	212.56	212.60	212.56	212.56
88	1.585	212.43	212.43	212.64	212.82
91	1.640	212.35	212.35	212.68	213.07
94	1.695	212.39	212.31	212.73	213.19
97	1.750	212.48	212.43	212.73	213.23
100	1.800	212.60	212.52	212.68	213.15
103	1.860	212.68	212.60	212.64	212.98
106	1.910	212.68	212.64	212.60	212.94
109	1.965	212.60	212.60	212.60	212.86
112	2.020	212.52	212.52	212.60	212.90
115	2.070	212.43	212.48	212.64	212.98
118	2.120	212.43	212.39	212.68	213.03
121	2.180	212.52	212.43	212.73	213.11
124	2.240	212.56	212.52	212.73	213.11
127	2.290	212.64	212.60	212.73	213.03
130	2.340	212.73	212.64	212.68	213.03

TABLE VII

Center Frequency Heights and Errors

Date of Test: 2nd March 1962

h_λ	Δh_λ	error	error	Δh_λ	error	error
	frequency increasing	percent	inches	frequency decreasing	percent	inches
0.20	0			0		
0.49						
0.76	0.56	12.0	3.34			
1.02				0.53	6.0	1.67
1.23	1.03	3.0	1.67			
1.56				1.07	7.0	3.89
1.76	1.56	4.0	3.33			
2.02				1.53	2.0	1.67
2.19	1.99	0.5	0.55			

Note: Errors were determined relative to heights derived from an expected height increment of 0.5λ , 27.8 inches at center frequency 212.5 megacycles per second.

Figure 1

Antenna over Reflecting Surface
and
Equivalent Image System

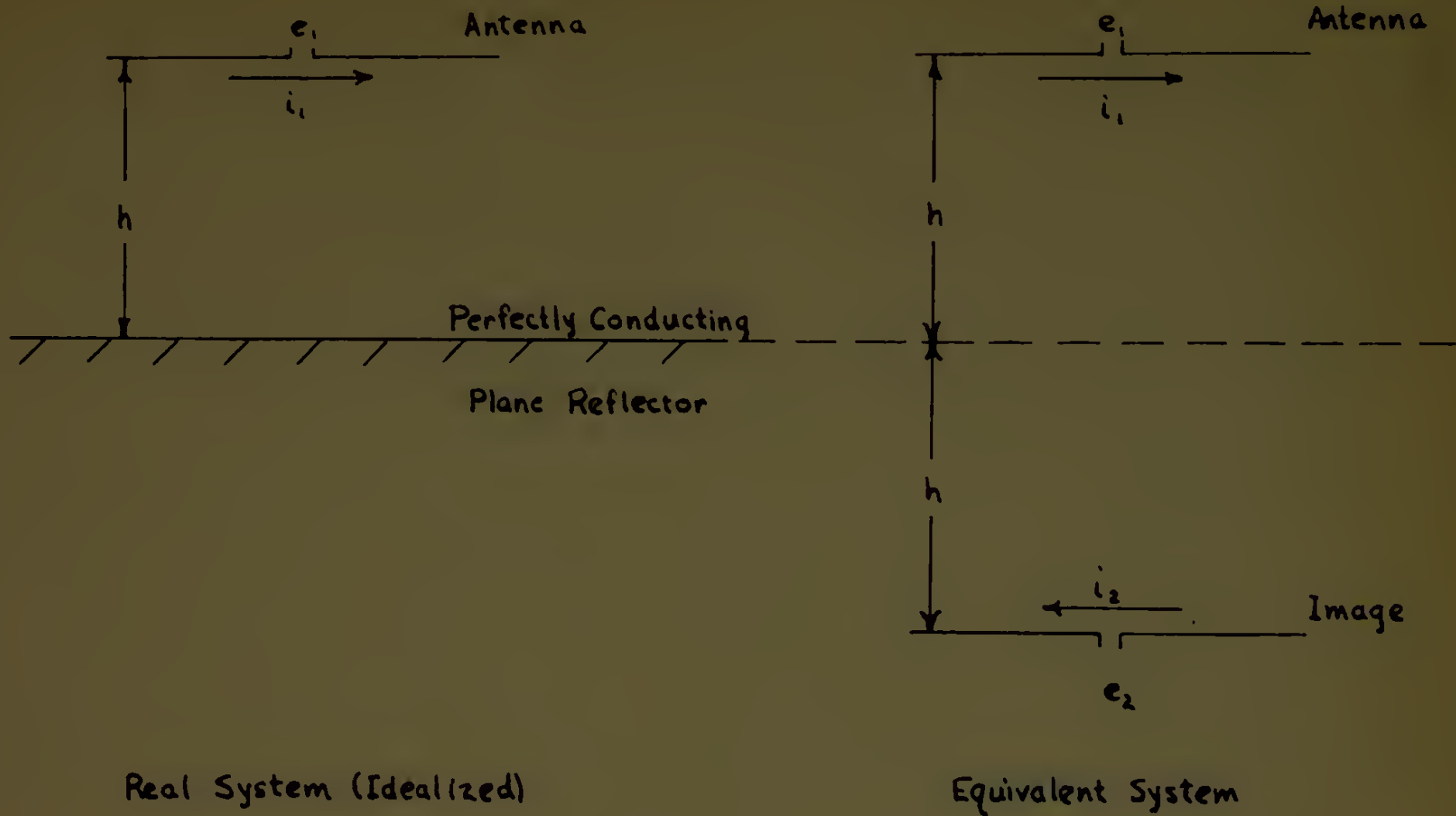


Figure 2
Input Admittance of
a Half-Wave Thin Dipole
over a Perfectly Conducting
Plane Reflecting Surface

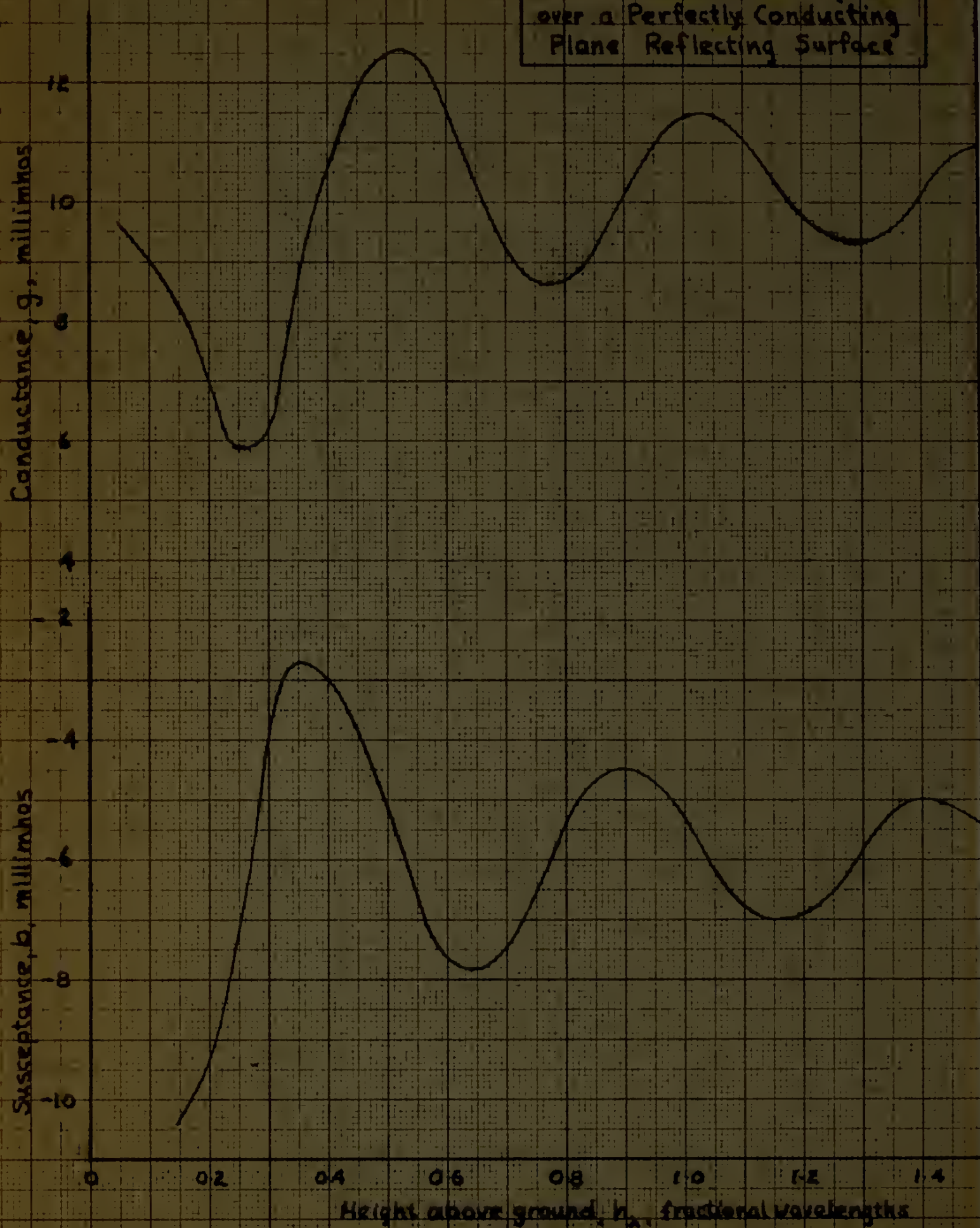
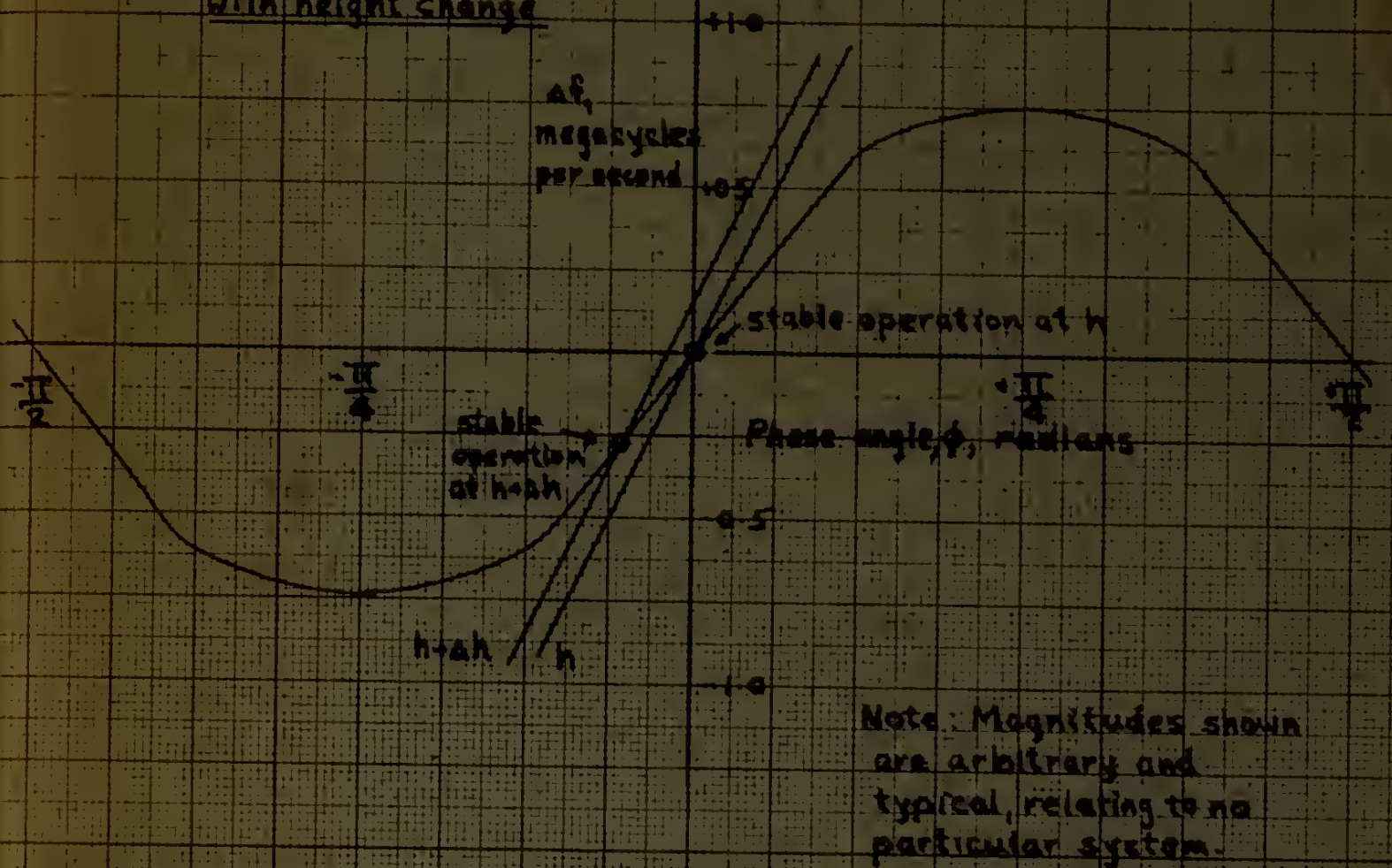
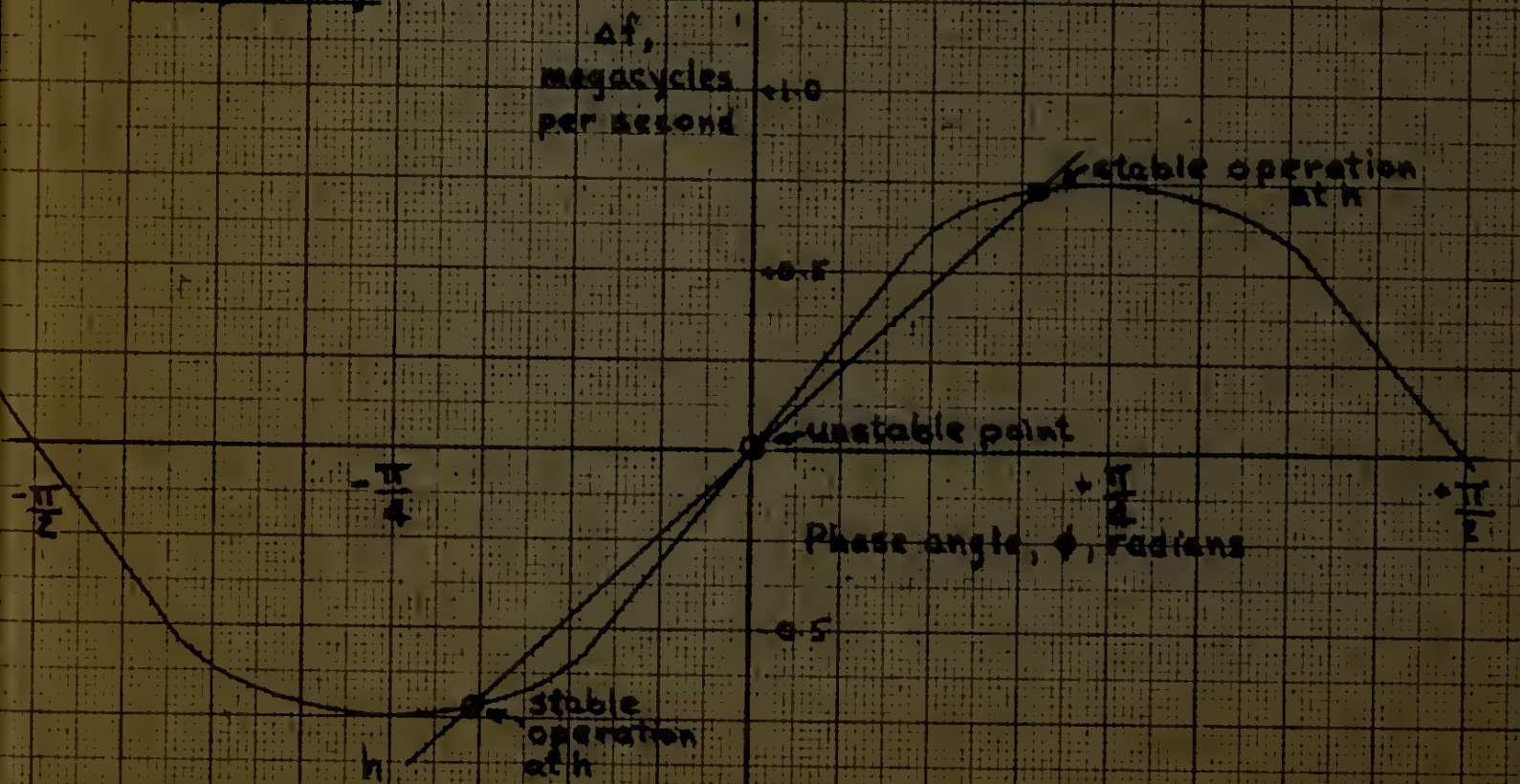


Figure 3
Dependence of
Oscillator Frequency
on Presented Load Phase

a. Pulling
with height change



b. Splitting



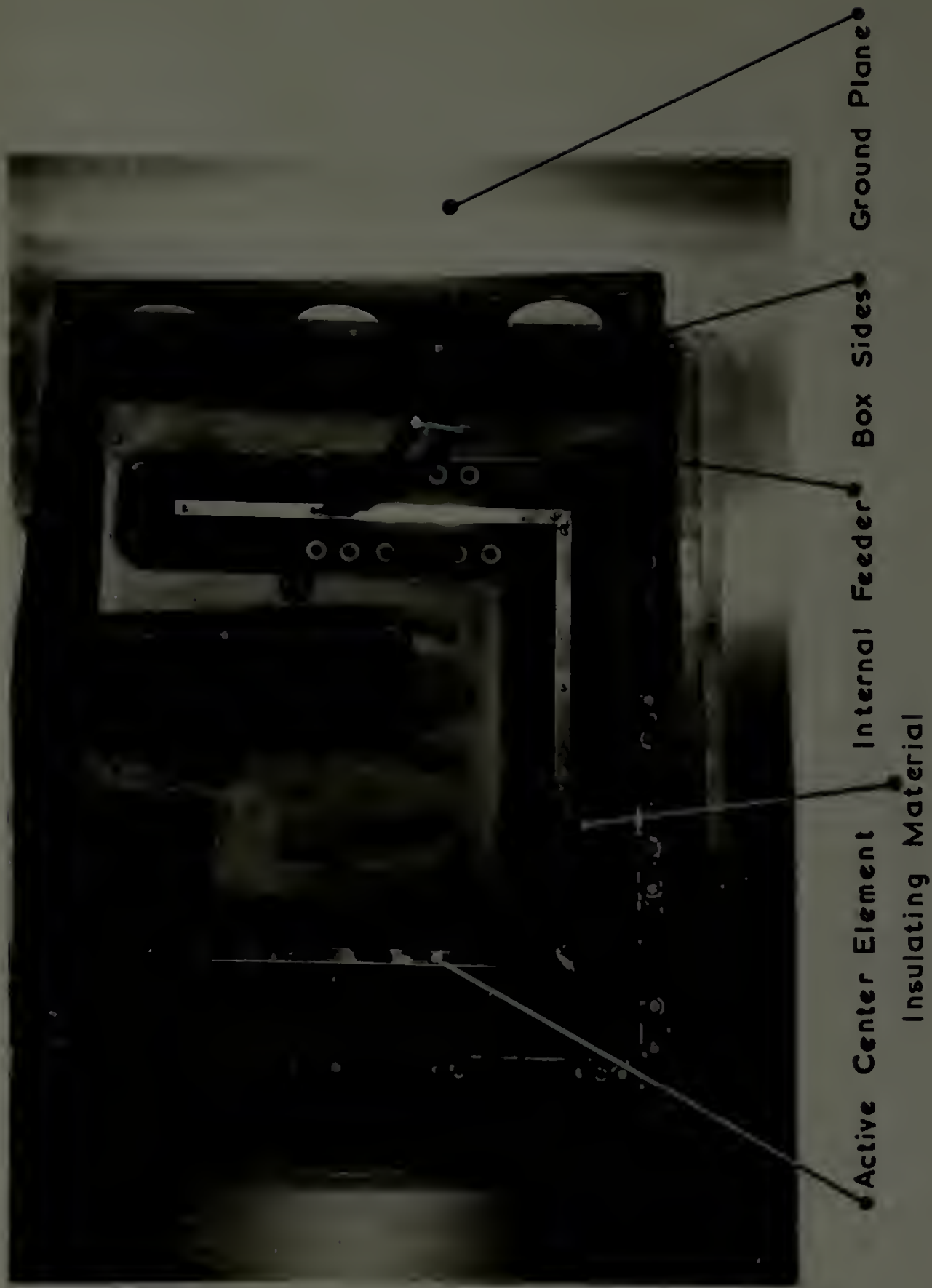
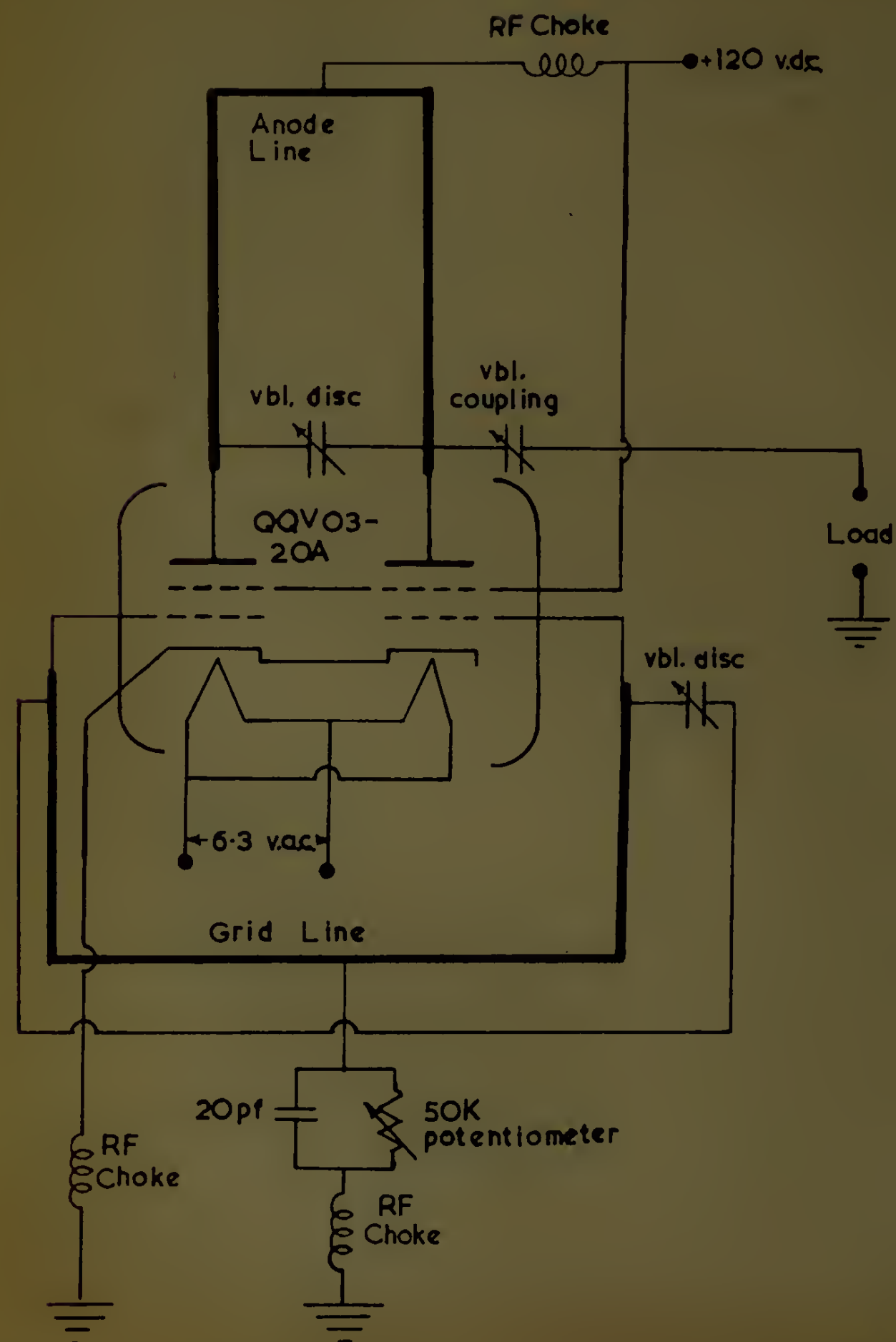


Figure 4 Rear Internal View of Antenna



Figure 5 Antenna: Radiating Face

Figure 6
Oscillator Schematic



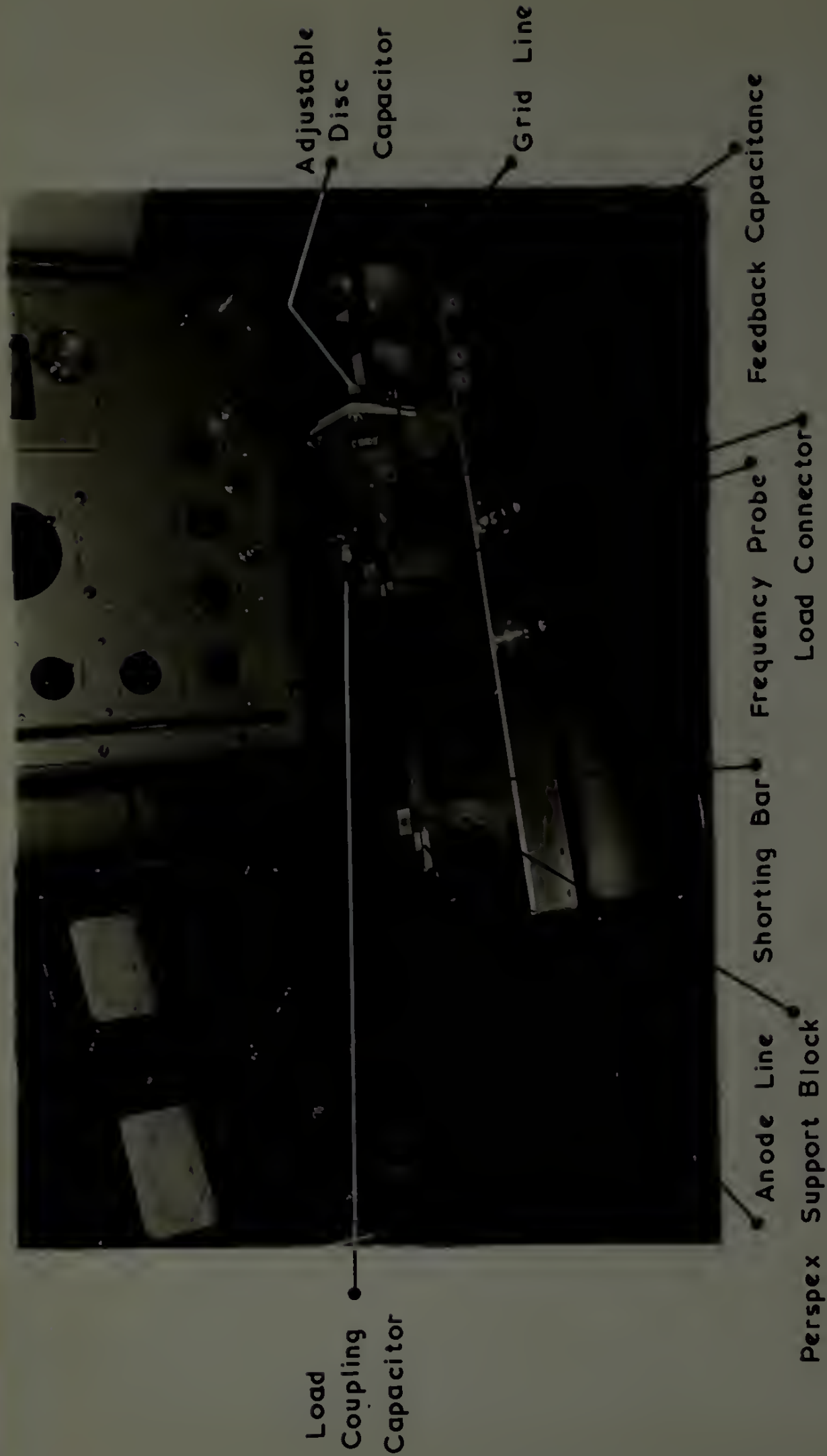


Figure 7 Tuned Line Oscillator

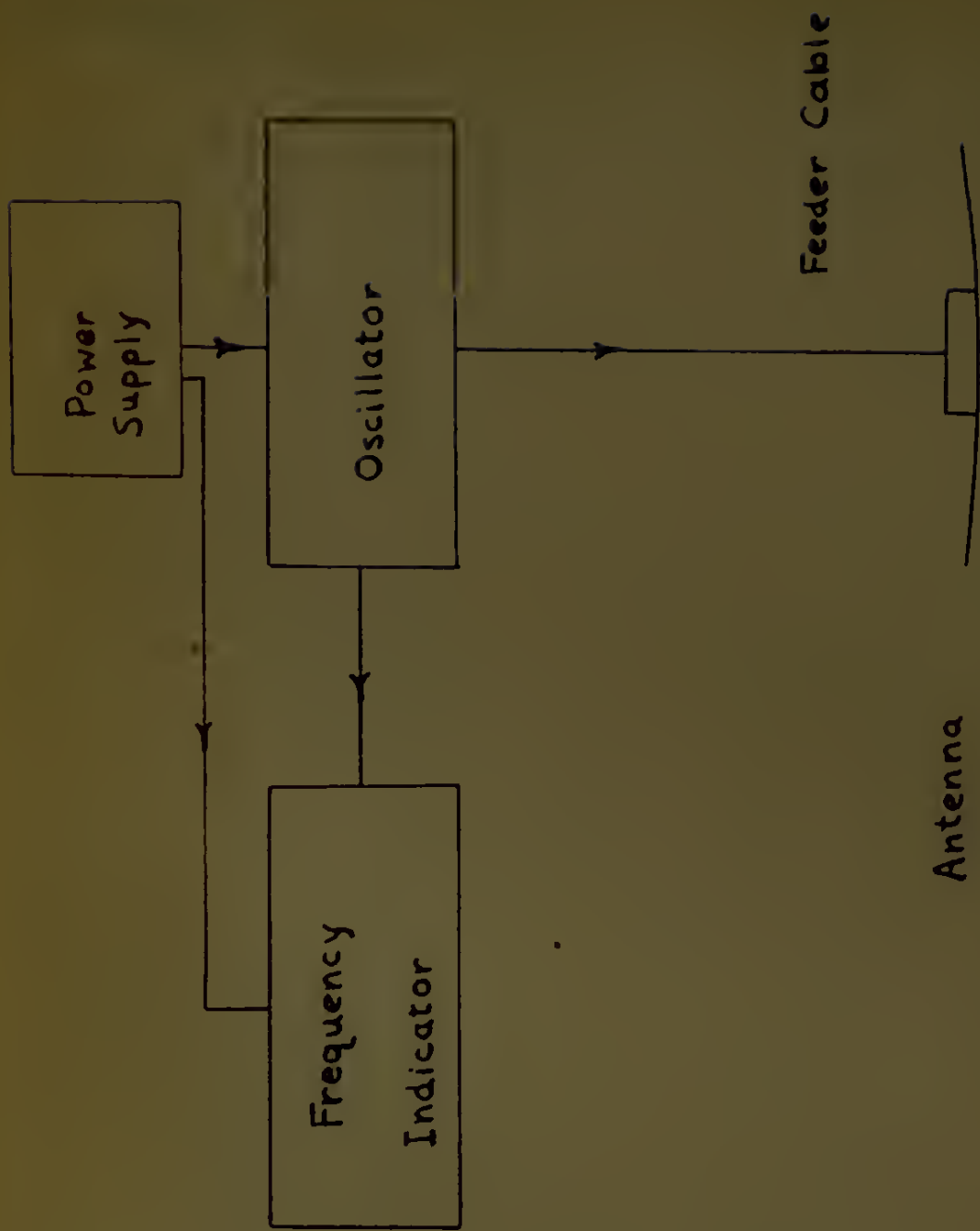


Figure 8
Block Diagram of
Experimental Height
Determining System

Reflecting Earth

225

220

215

210

205

200

195

190

18.0

19.0

20.0

21.0

22.0

23.0

24.0

25.0

26.0

27.0

28.0

Injected Signal Frequency, megacycles per second

Logging Scale Indication when Tuned

Figure 9

Airmec 248 Wave Analyser
Calibration Curve

CPB 2-62

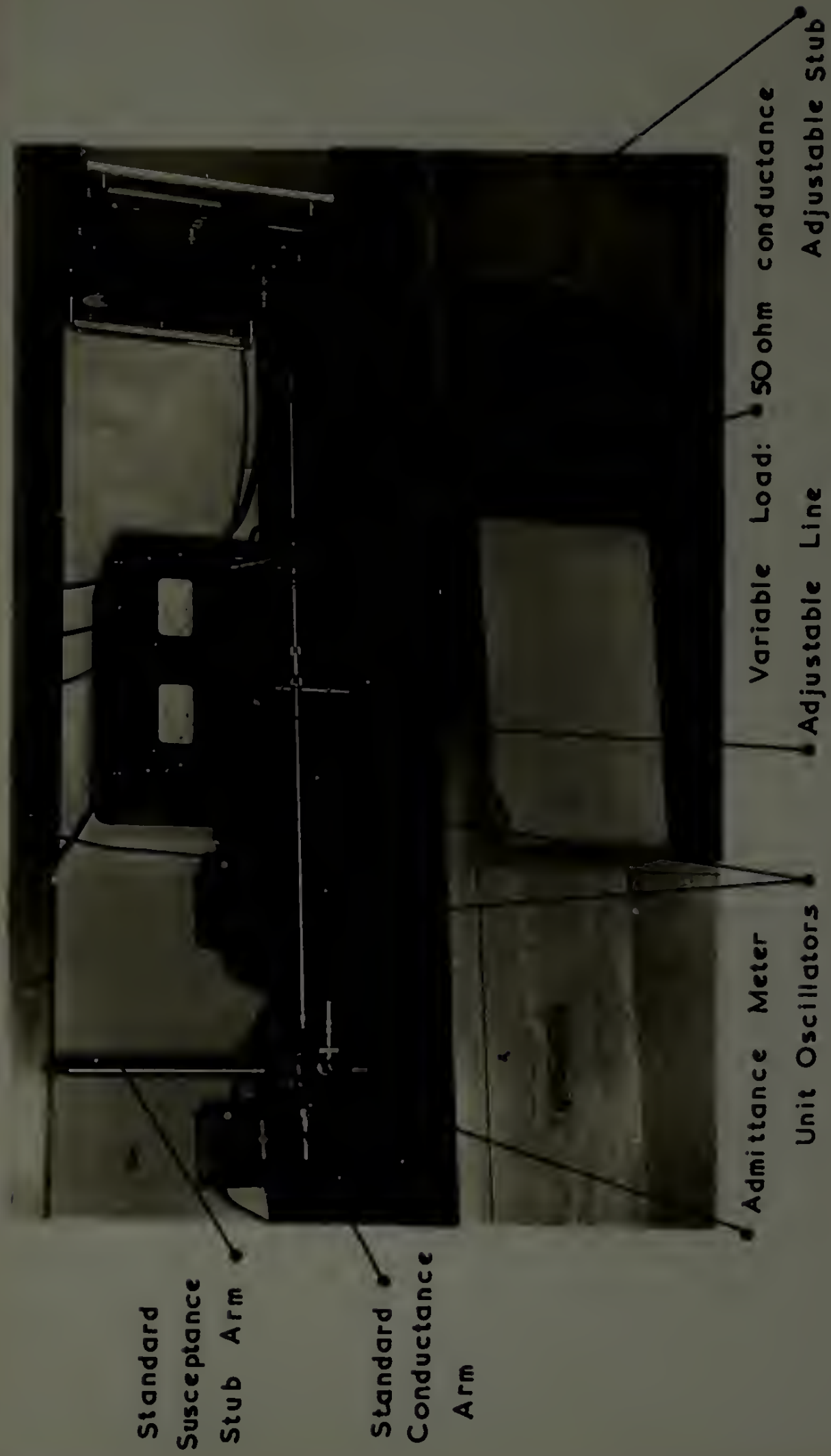


Figure 10 G. R. Admittance Meter and Variable Test Load



Figure II
Antenna and Suspension Rig
as Viewed from the Ground



Figure 12 Suspended Antenna and Cable
Viewed from Above



Disruptive Reflecting Surface

Figure 13 Fence Stakes

ADMITTANCE COORDINATES—20-MILLIMHO CHARACTERISTIC ADMITTANCE

Note: Frequencies shown are in megacycles/sec.

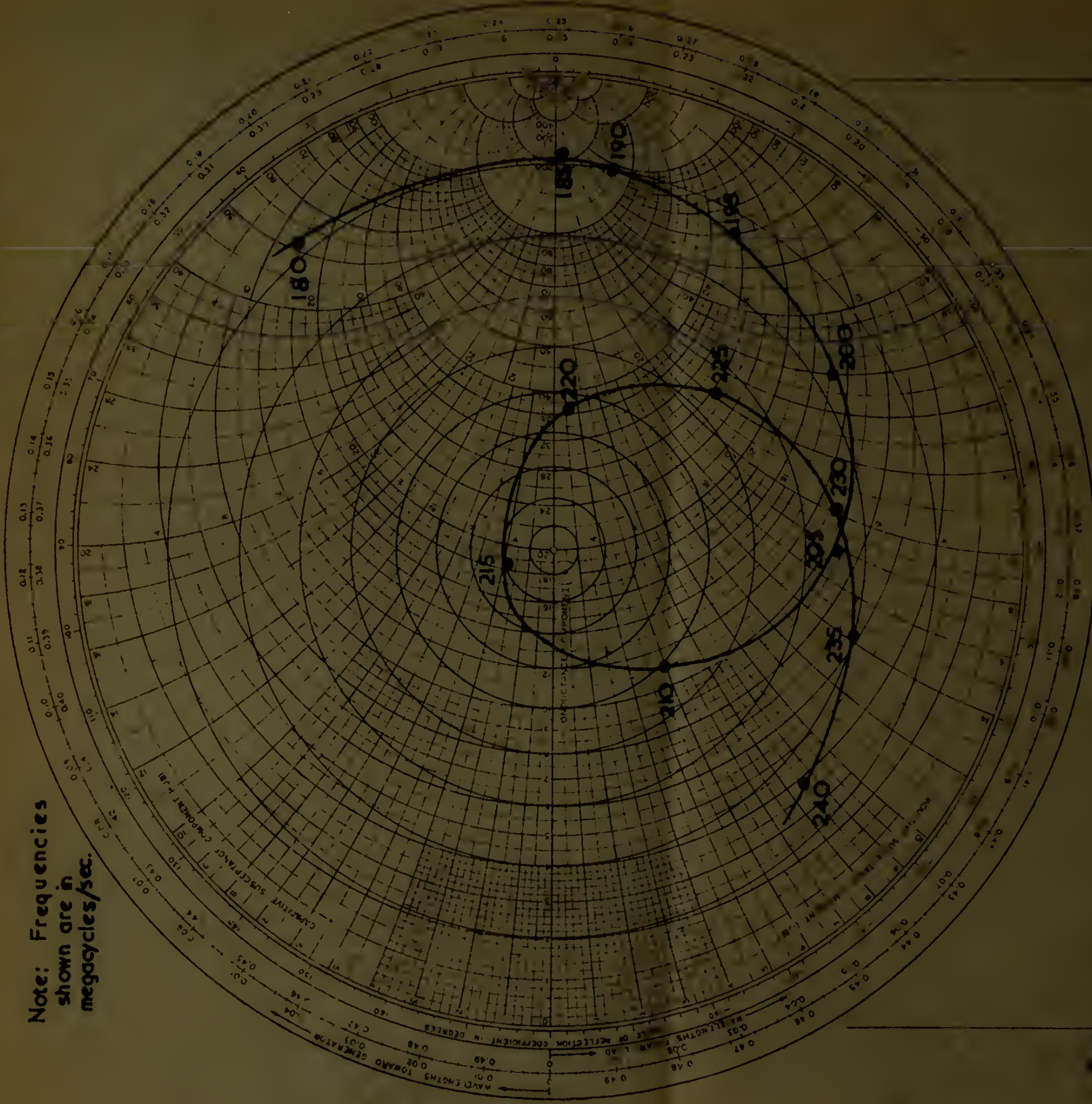


FIG.

TITLE Line Oscillator Rieke Diagram

NO. 15

GENERAL RADIO COMPANY, CAMBRIDGE, MASSACHUSETTS

DATE 1-62

Center Frequency: 207 mc/s.
IMPEDANCE OR ADMITTANCE COORDINATES

Note: Frequency contours solid, with points alternately open and filled. Power contours dashed. Frequencies shown in mega-cycles/second.

ctg

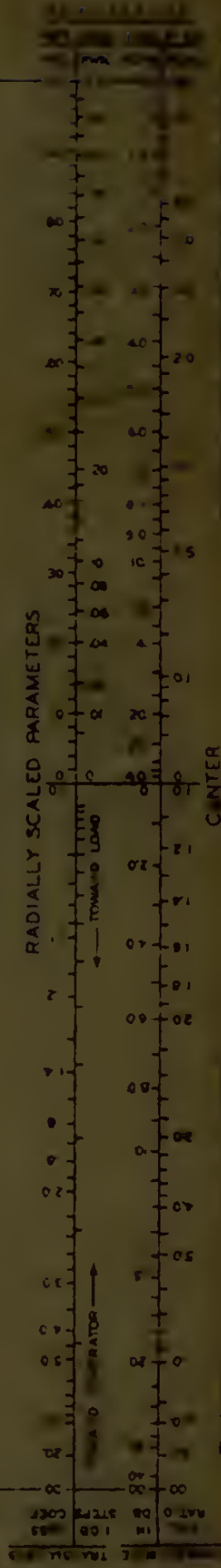


NAME	TITLE Line Oscillator Rieke Diagram (modified)		FIG. NO. 16
SMITH CHART	showing effect of variation of coupling to load		DATE 2-62
GENERAL RADIO COMPANY, CAMBRIDGE, MASSACHUSETTS			

Center frequency: 210 mc./s.
IMPEDANCE OR ADMITTANCE COORDINATES

Note: Frequencies shown are in megacycles/second.

Key: tight coupling, capacitor fully in
 — mid coupling, one turn out
 --- loose coupling, capacitor fully out



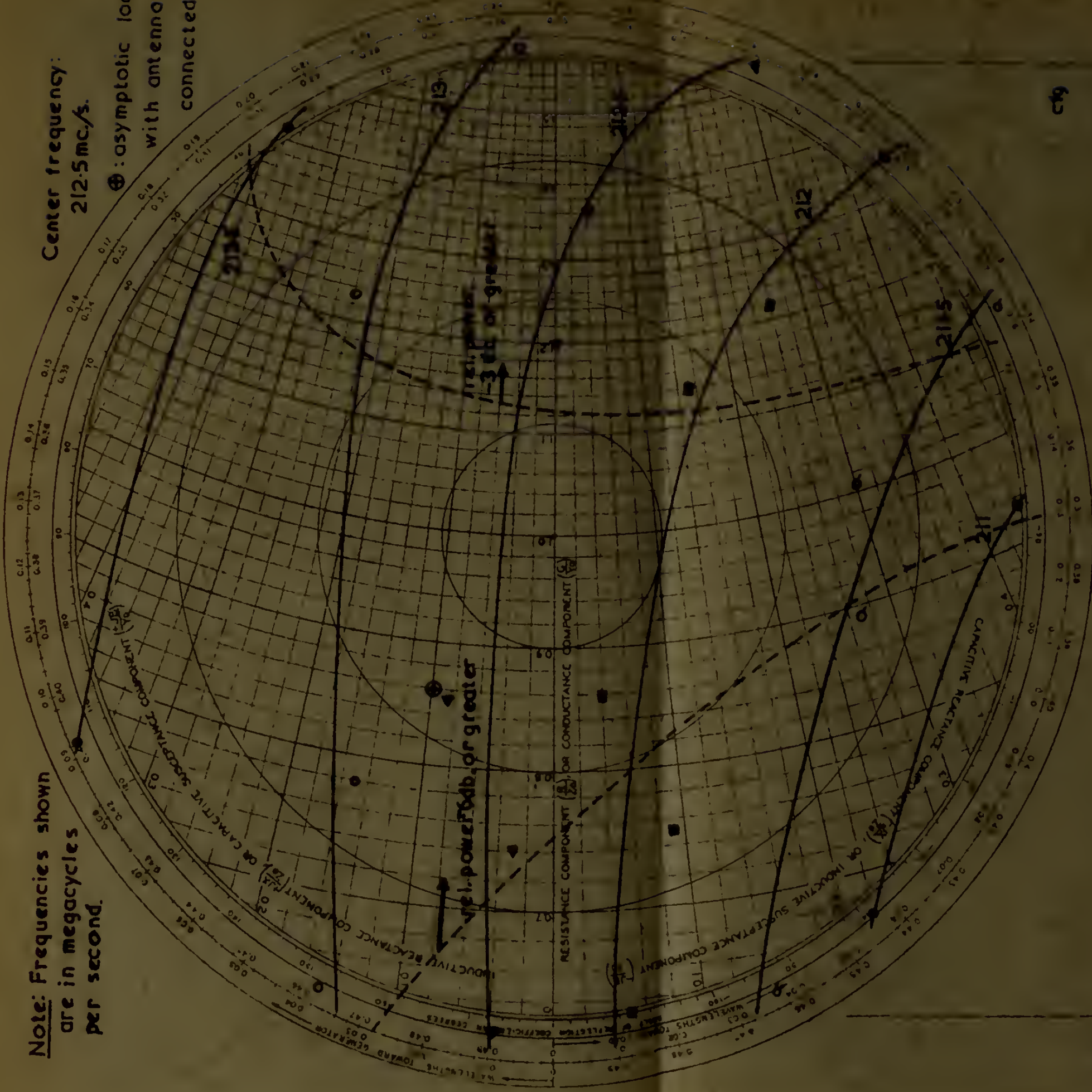
NAME	TITLE	FIG. NO.
SMITH CHART	Line Oscillator Rieke Diagram (partial)	17
Form 756-NE	GENERAL RADIO COMPANY, CAMBRIDGE, MASSACHUSETTS	DATE
		2-62

IMPEDANCE OR ADMITTANCE COORDINATES

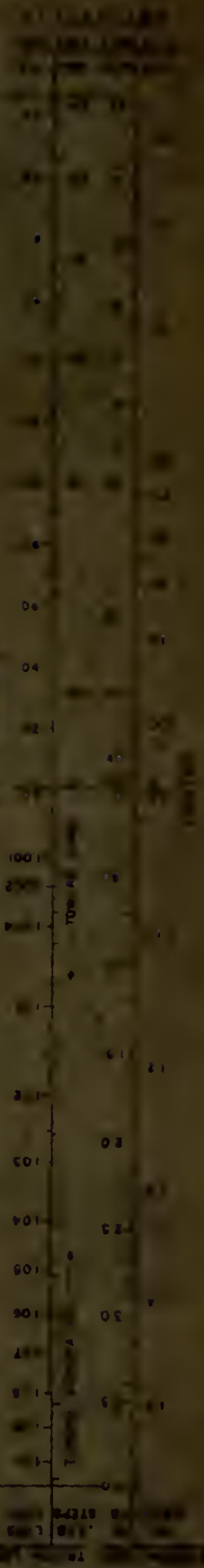
Note: Frequencies shown are in megacycles per second.

Center frequency:
212.5mc./s.

⊕: asymptotic load with antenna connected.



RADIALLY CALLED PARAMETERS



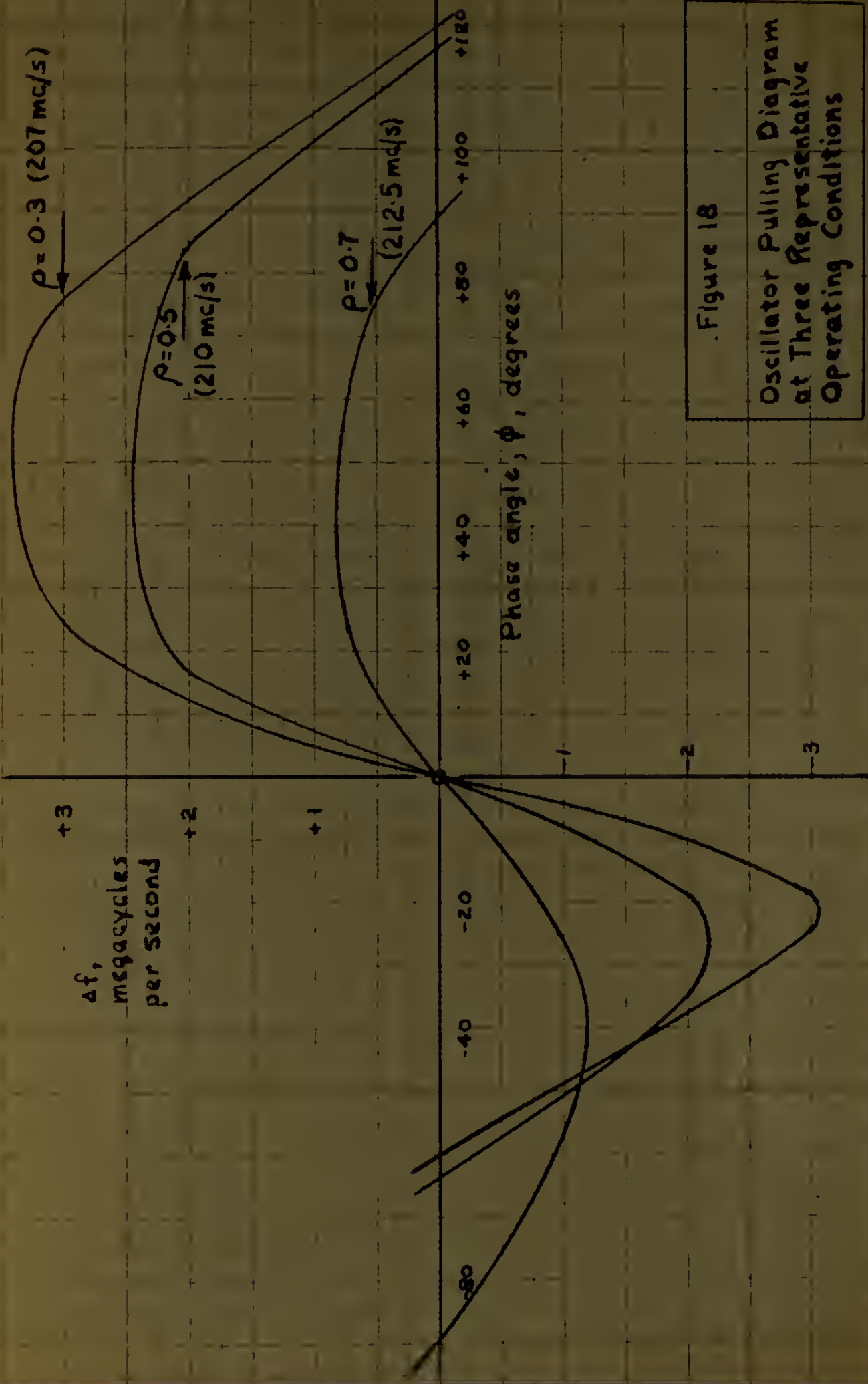
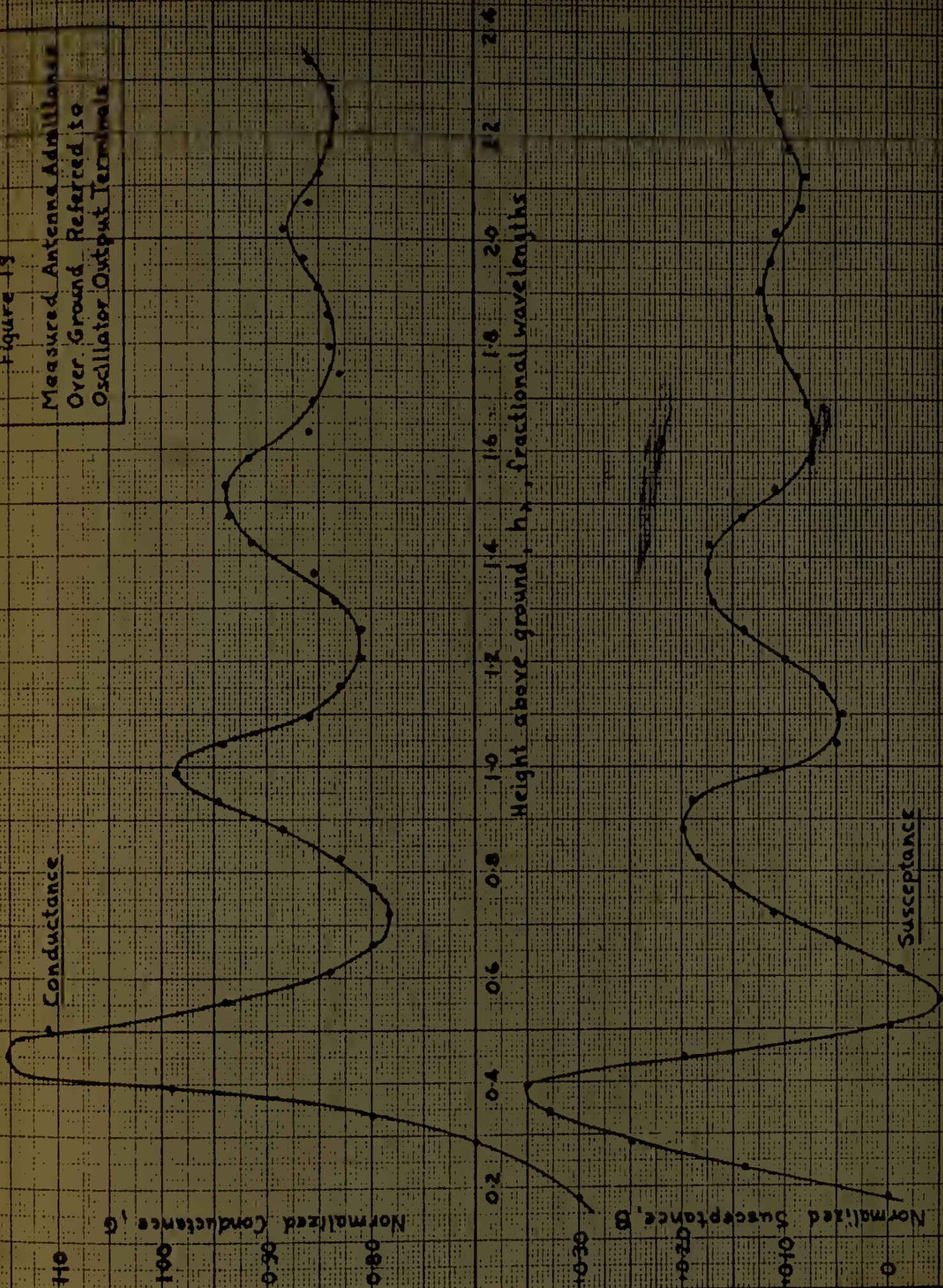


Figure 18

Oscillator Pulling Diagram
at Three Representative
Operating Conditions

Figure 13

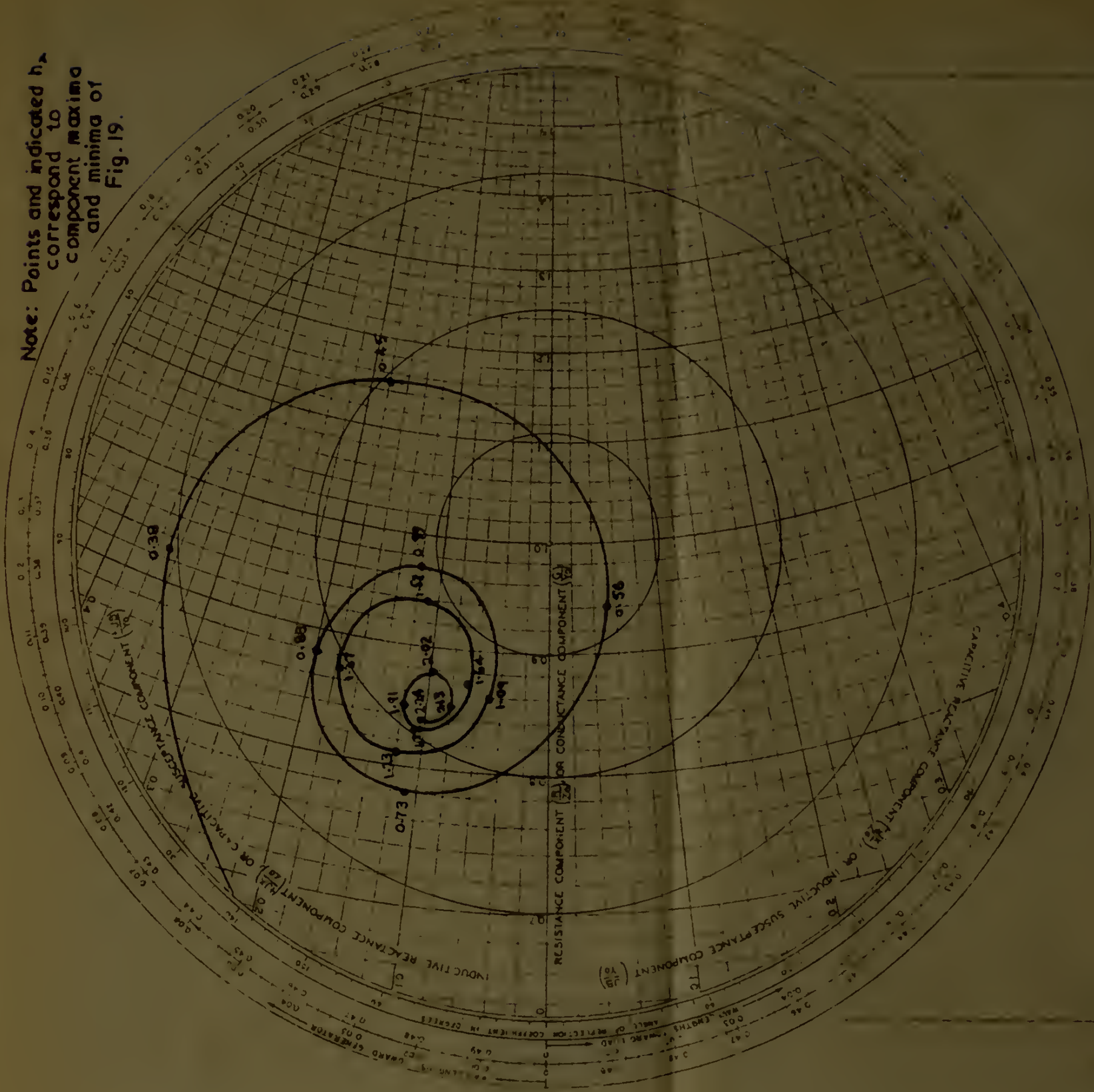
Measured Antenna Admittance
Over Ground Referred to
Oscillator Output Terminals



NAME C.F. Gerhan	TITLE Measured Antenna Admittance over Ground Referred to Oscillator Output Connector	FIG. NO. 20
SMITH CHART Form 756-NE	GENERAL RADIO COMPANY, CAMBRIDGE, MASSACHUSETTS	DATE 3-62

IMPEDANCE OR ADMITTANCE COORDINATES

Note: Points and indicated h_p correspond to component maxima and minima of Fig. 19.



WAVELENGTHS TOWARD GENERATOR	WAVELENGTHS TOWARD LOAD	ANGLE OF REFLECTION COEFFICIENT IN DEGREES	ANGLE OF TRANSMISSION COEFFICIENT IN DEGREES	SWR	LOSS COEFF	LOSS DB	ATTEN DB	ATTEN DB	ATTEN DB
0.00	0.00	0	0	1.00	0.00	0.00	0.00	0.00	0.00
0.01	0.01	3.6	3.6	1.02	0.01	0.04	0.04	0.04	0.04
0.02	0.02	7.2	7.2	1.04	0.02	0.08	0.08	0.08	0.08
0.03	0.03	10.8	10.8	1.06	0.03	0.12	0.12	0.12	0.12
0.04	0.04	14.4	14.4	1.08	0.04	0.16	0.16	0.16	0.16
0.05	0.05	18.0	18.0	1.10	0.05	0.20	0.20	0.20	0.20
0.06	0.06	21.6	21.6	1.12	0.06	0.24	0.24	0.24	0.24
0.07	0.07	25.2	25.2	1.14	0.07	0.28	0.28	0.28	0.28
0.08	0.08	28.8	28.8	1.16	0.08	0.32	0.32	0.32	0.32
0.09	0.09	32.4	32.4	1.18	0.09	0.36	0.36	0.36	0.36
0.10	0.10	36.0	36.0	1.20	0.10	0.40	0.40	0.40	0.40

SWR	LOSS COEFF	LOSS DB	ATTEN DB	ATTEN DB	ATTEN DB
1.00	0.00	0.00	0.00	0.00	0.00
1.02	0.01	0.04	0.04	0.04	0.04
1.04	0.02	0.08	0.08	0.08	0.08
1.06	0.03	0.12	0.12	0.12	0.12
1.08	0.04	0.16	0.16	0.16	0.16
1.10	0.05	0.20	0.20	0.20	0.20
1.12	0.06	0.24	0.24	0.24	0.24
1.14	0.07	0.28	0.28	0.28	0.28
1.16	0.08	0.32	0.32	0.32	0.32
1.18	0.09	0.36	0.36	0.36	0.36
1.20	0.10	0.40	0.40	0.40	0.40

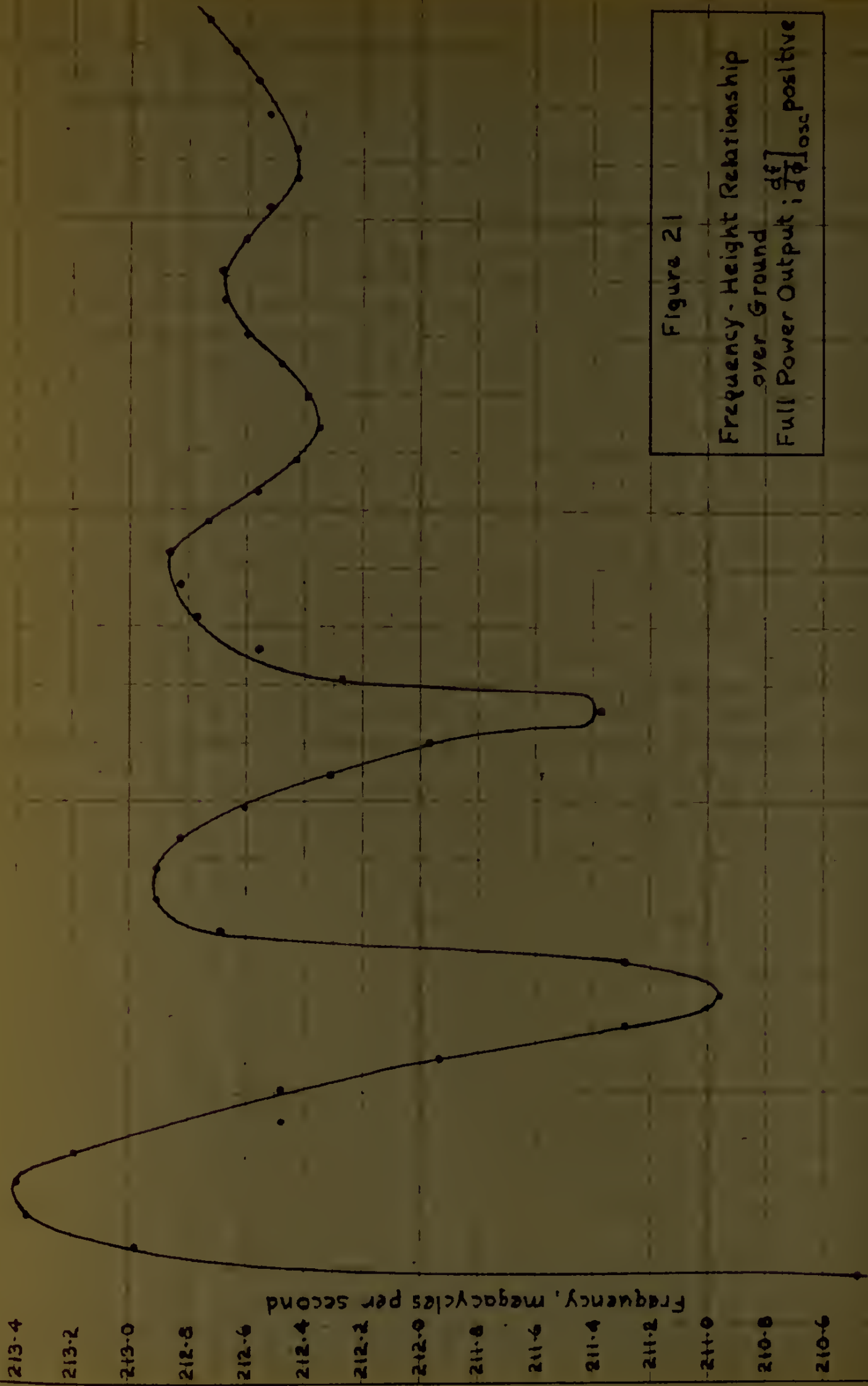


Figure 21

Frequency-Height Relationship
 over Ground
 Full Power Output; $\frac{d\phi}{d\theta}$ positive

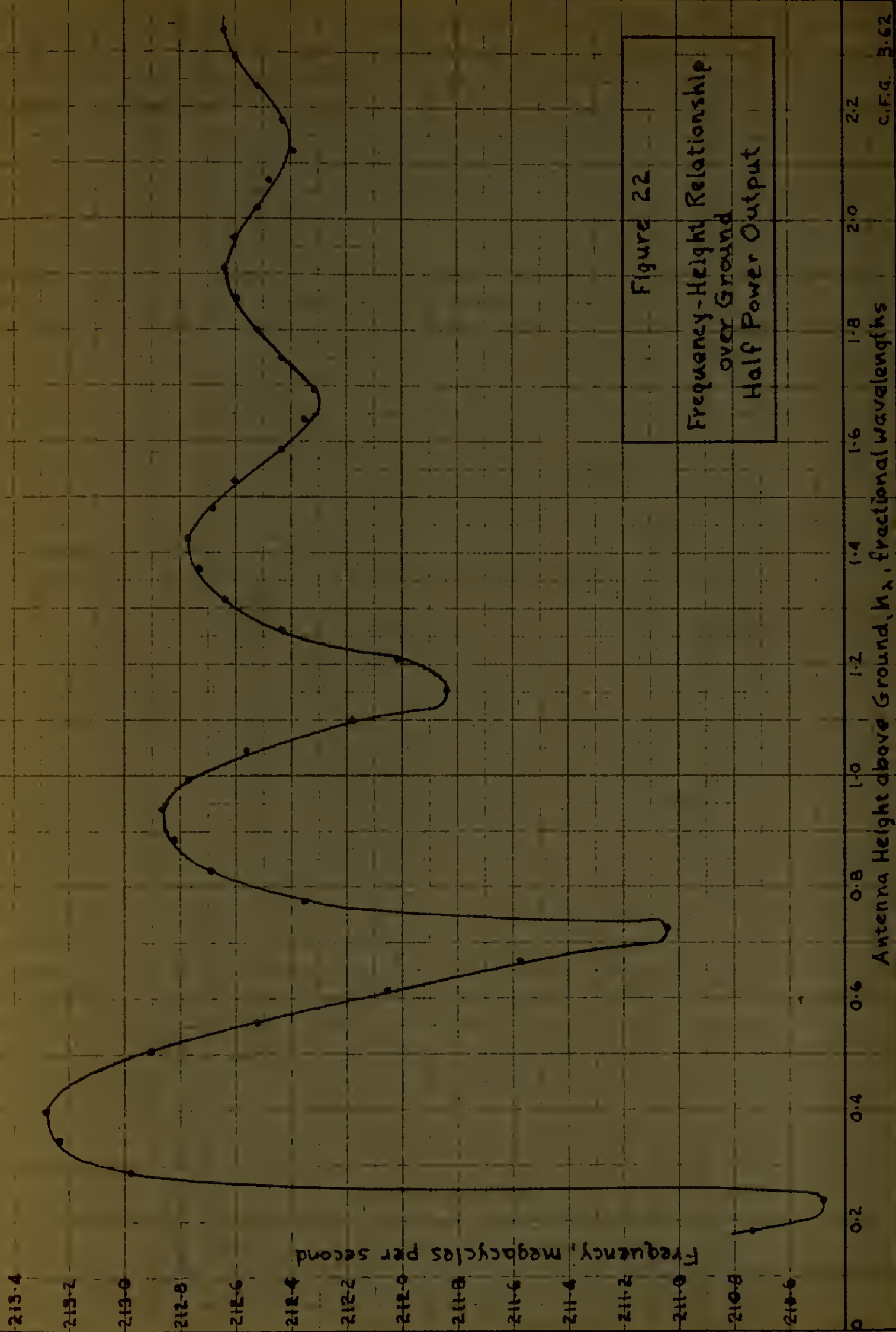


Figure 22

Frequency-Height Relationship
over Ground
Half Power Output

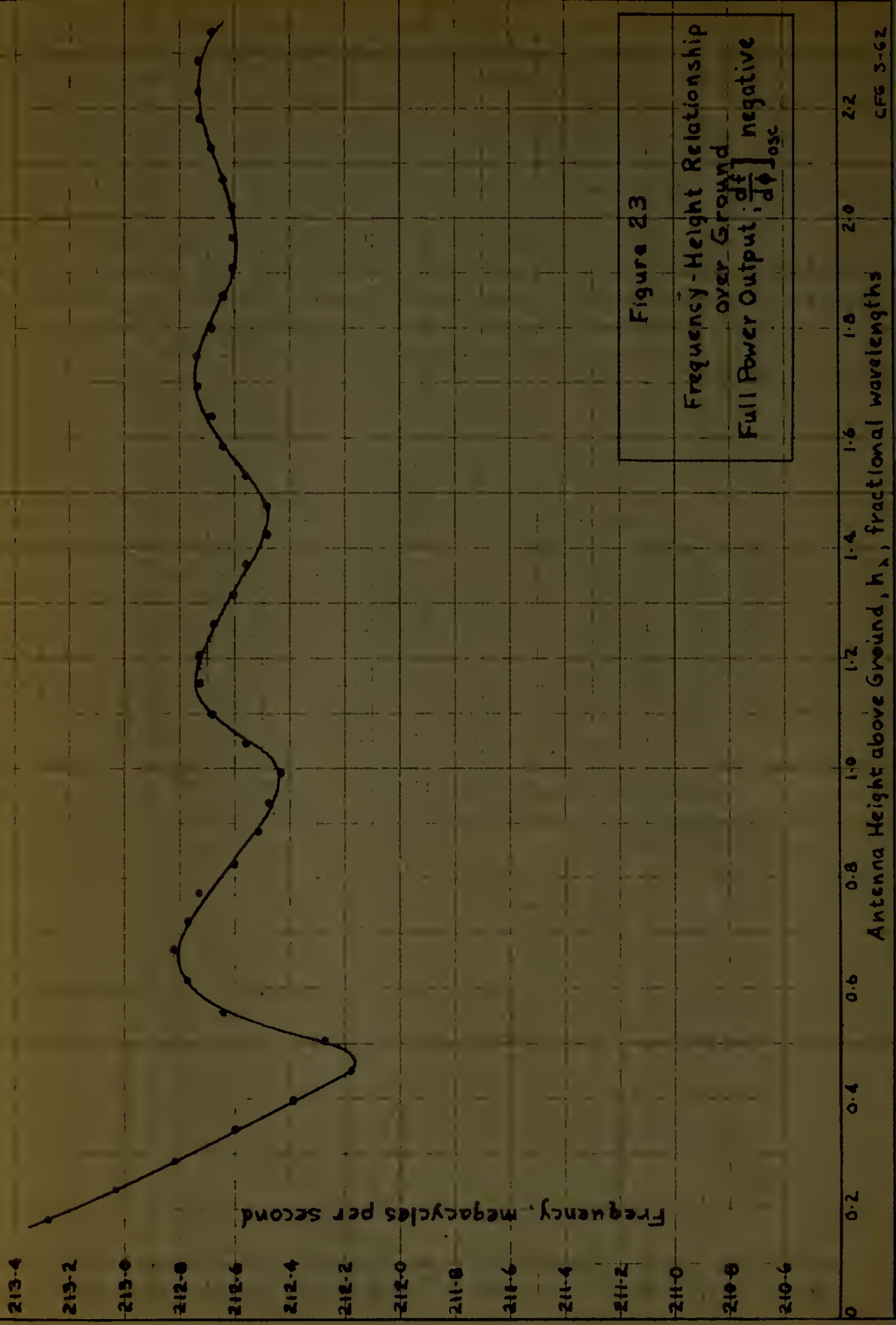
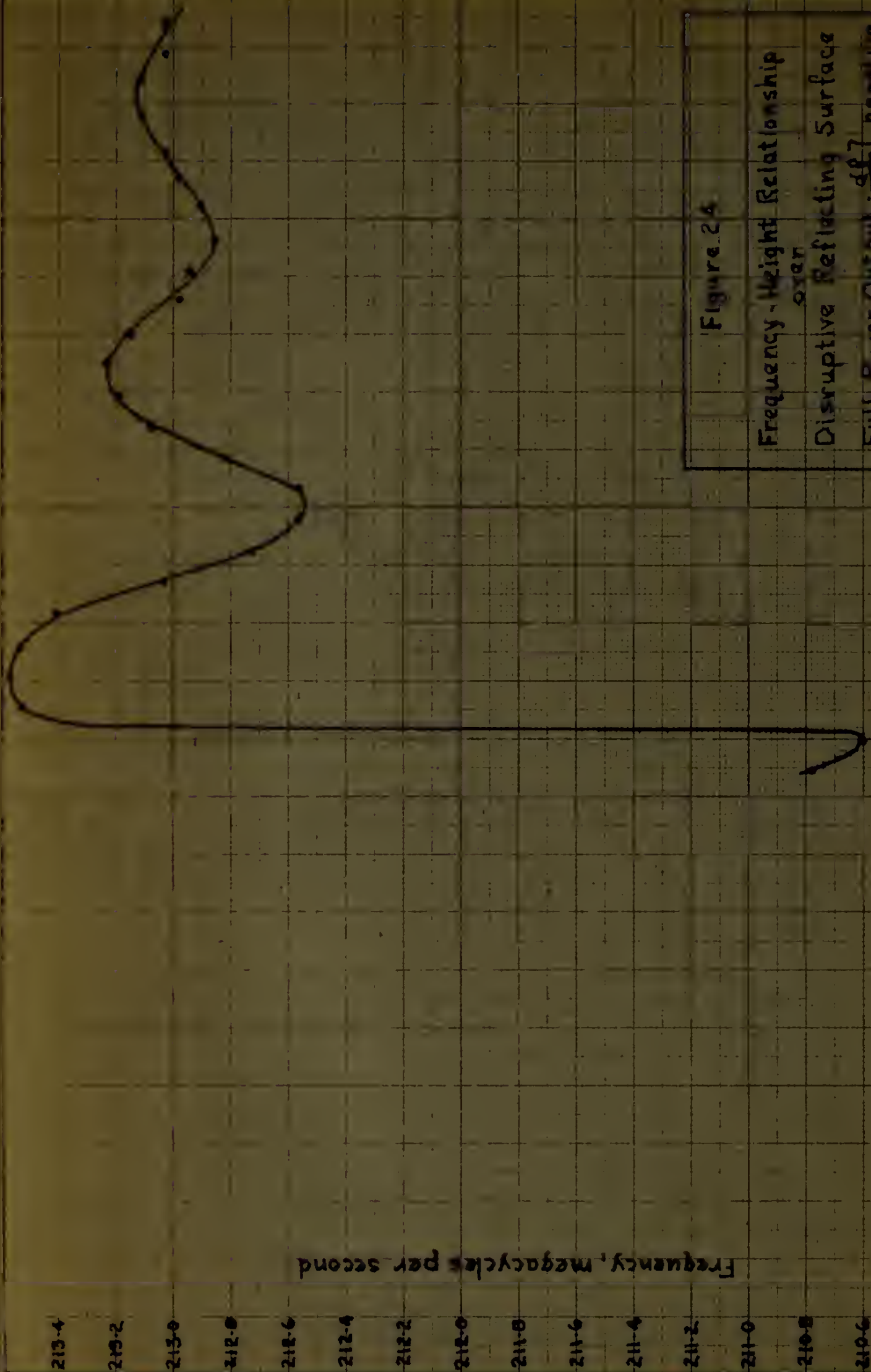


Figure 23

Frequency-Height Relationship
over Ground
Full Power Output; $\left[\frac{d\phi}{d\phi} \right]_{osc}$ negative



Frequency, megacycles per second

0.2

0.4

0.6

0.8

1.0

1.2

1.4

1.6

1.8

2.0

2.2

0

Antenna Height above Ground, h_p , fractional wavelengths

Figure 2A

Frequency-Height Relationship
Disruptive Reflecting Surface
Full Power Output; $\left[\frac{dP}{d\theta}\right]_{\theta=0}$ negative

3-62

Note:

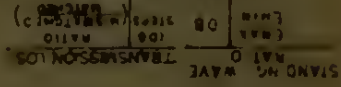
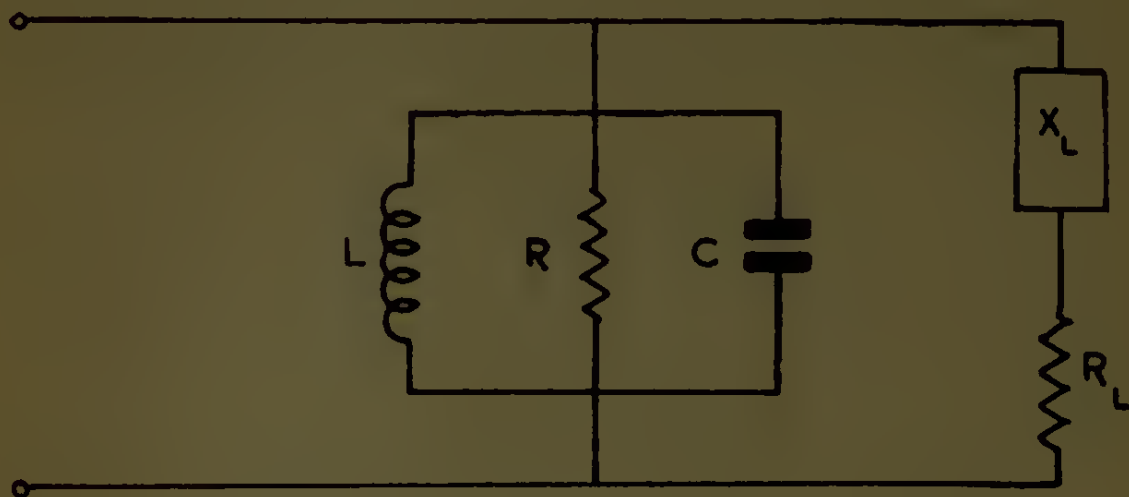
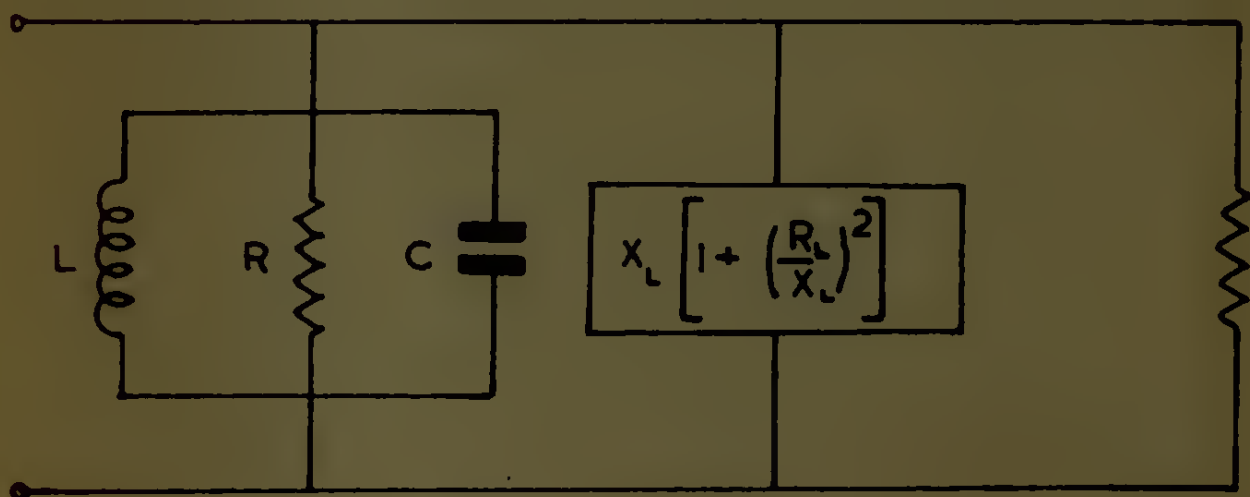


Figure 26
Simple Loaded Oscillator
and Equivalent Circuit



26 a



26 b

$$R_L \left[1 + \left(\frac{X_L}{R_L} \right)^2 \right]$$

thesG295

A simplified approach to low height dete



3 2768 002 02595 9

DUDLEY KNOX LIBRARY